Abundance determinations in H II regions and planetary nebulae

By GRAŻYNA STASIŃSKA

Observatoire de Paris-Meudon, 5, place Jules Janssen, 92195 Meudon cedex, France

The methods of abundance determinations in H II regions and planetary nebulae are described, with emphasis on the underlying assumptions and inherent problems. Recent results on abundances in Galactic H II regions and in Galactic and extragalactic Planetary Nebulae are reviewed.

H II regions are ionized clouds of gas associated with zones of recent star formation. They are powered by one, a few, or a cluster of massive stars (depending on the resolution at which one is working). The effective temperatures T_{\star} of the ionizing stars lie in the range 35 000 – 50 000 K. The nebular geometries result from the structure of the parent molecular cloud. Stellar winds, at evolved stages, may produce ring-like structures, but the morphology of H II regions is generally rather complex on all scales. Typical hydrogen densities n are $10^3 - 10^4$ cm⁻³ for compact H II regions. The average densities in giant extragalactic H II regions are lower, typically 10^2 cm⁻³ since giant H II regions encompass also zones of diffuse material. The total supply of nebular gas is generally large, so that all (or at least a significant fraction) of the ionizing photons are absorbed.

Planetary nebulae (PNe) are evolutionary products of so-called intermediate mass stars (initial masses of $1 - 8 M_{\odot}$) as they progress from the asymptotic giant branch (AGB) to the white dwarf stage. It is the interaction of the slow AGB wind with the fast post-AGB wind which produces the nebula. Because the ionizing star is also the remnant of the PN progenitor, the morphology is much simpler that in the case of H II regions, although not all PNe are round! The temperature of the central star – or nucleus – can be much higher than that of main sequence massive stars, reaching values of the order 200000 K for a remnant of about 0.6 M_☉. The densities of the brightest (and therefore best studied) PNe are around $10^3 - 10^5$ cm⁻³. PNe of lower densities, corresponding to more evolved stages, are fainter and therefore less observed. The amount of nebular gas is not always sufficient to trap all the stellar ionizing photons, and a significant part of these may leak out from the nebula.

This brief introduction points at two things. One is that the ionized plasmas in H II regions and PNe are similar from the physical point of view, and therefore can be analyzed with similar techniques (although the range of physical conditions is somewhat different). The other is that the astrophysical significance of the chemical composition in these two classes of objects is not the same. H II regions probe the state of the gas at the birth of massive stars (i.e. a few Myr ago). The status of the chemical composition of PN envelopes is more complex. Some constituents have not been changed and reflect the state of the gas out of which the progenitor of the PN was formed, 10⁸ yr ago or more. Other elements, such as carbon and nitrogen, have had their abundances strongly affected by nucleosynthesis and mixing processes in the progenitor, and therefore probe the evolution of intermediate mass stars.

The text presented below is based on lectures given at the XIII Canary Islands Winterschool on Cosmochemistry, where I have been asked to review the status of abundances in planetary nebulae (both Galactic and extragalactic) and in Galactic H II regions. Abundances in extragalactic H II regions were treated by Don Garnett, and the determination of the primordial helium abundance using low metallicity H II galaxies was discussed by

Gary Steigman. In my lectures, I have emphasized the methods for abundance determinations in ionized nebulae. In this respect, giant extragalactic H II regions provide interesting complementary information and methods used for giant H II regions were included for completeness.

The scope of this article is as follows. Section 1 summarizes the basic physics of photoionized nebulae, Section 2 presents the different families of methods for abundance determinations. Section 3 discusses the various sources of uncertainties. Section 4 outines some important recent results on abundances in the Milky Way H II regions, including ring nebulae. Section 5 presents a selection of recent results on abundances in planetary nebulae, that are relevant to our understanding of the chemical history of galaxies or of the nucleosynthesis in intermediate mass stars. Due to limited space (and limited knowledge!), Sections 4 and 5 are not to be taken for extensive reviews. A large amount of interesting work could not be mentioned here. This text is rather to be understood as a guide line for the astronomer interested in nebular abundances, either to embark on his own abundance determinations or to be able to better understand the literature on this topic. The papers quoted below were preferably chosen among recent studies published in refereed journals. A few pioneering, older studies are occasionally mentioned.

1. Basic physics of photoionized nebulae

Excellent introductions are provided in textbooks such as those of Spitzer (1978), Aller (1984) or Osterbrock (1989). Here, we simply emphasize the properties to bear in mind when dealing with abundance determinations.

1.1. Ionization and recombination

1.1.1. Global ionization budget

2

Consider a source of photons surrounded by a cloud of nebular gas. The gas particles are ionized by those photons with energies above the ionization threshold. Once ionized, the particles tend to recombine with the free electrons, and an equilibrium stage is eventually established in which the rate of ionization equals the rate of recombination for each species.

Closer to the source, the density of ionizing photons is larger, therefore the resulting ionization state of the gas is higher. If there is enough nebular matter, all the ionizing photons can be absorbed, producing an ionization bounded nebula. If not, the nebula is called density bounded.

It is the most abundant species, (H and He in general, but this could be C, N, O in hydrogen-poor material) which absorb most of the Lyman continuum photons from the ionizing source, and thus define the size of the ionized region in the ionization bounded case.

In an ionization bounded nebula purely composed of hydrogen, the total number of recombinations per unit time balances the total number of photons with energies above 13.6 eV emitted per unit time either by the star, or during recombination to the ground level. One has:

$$Q(\mathbf{H}^0) + \int n(\mathbf{H}^+) n_e \epsilon \alpha_1(\mathbf{H}, T_e) dV = \int n(\mathbf{H}^+) n_e \epsilon \alpha_{tot}(\mathbf{H}, T_e) dV, \qquad (1.1)$$

where $Q(\mathrm{H}^0)$ is the total number of photons with energies above 13.6 eV emitted by the star per second; $n(\mathrm{H}^+)$ is the number density of H ions, n_e is the electron density, ϵ is the volume filling factor of the nebular gas; $\alpha_1(\mathrm{H}, T_e)$ is the H recombination coefficient to the ground level while $\alpha_{tot}(\mathbf{H}, T_e)$ is the total H recombination coefficient, which are both roughly inversely proportional to the electron temperature T_e . The integrations are performed over the nebular volume.

In the case of a constant density nebula with constant filling factor, the radius of the ionized region, or Strömgren radius is then:

$$R_S = \left(\frac{3Q(\mathrm{H}^0)}{4\pi\epsilon n_e^2 \alpha_B(\mathrm{H}, T_e)}\right)^{1/3},\tag{1.2}$$

where $\alpha_B(\mathbf{H}, T_e)$ is the H recombination coefficient to the excited states (in this equation, T_e represents an average electron temperature of the nebula). The thickness of the transition region between the fully ionized zone and the neutral zone is approximately one mean free path of an ionizing photon $d = 1/n(\mathbf{H}^0)\alpha_{\nu}$, where α_{ν} is the hydrogen photoionization cross section at the typical frequency of the photons reaching the ionization front. This thickness is generally much smaller than the size of the nebula and justifies the concept of a Strömgren sphere. There are however cases when the transition region might be extended, such as in diffuse media or when the ionizing radiation field contains a large amount of X-ray photons (which are less efficiently absorbed by hydrogen).

During the recombination process captures to the excited levels decay to lower levels by radiative transitions. The total luminosity of the H β line is thus

$$L_{\mathrm{H}\beta} = \int n(\mathrm{H}^+) n_{\mathrm{e}} \epsilon 4\pi j_{\mathrm{H}\beta}(T_e) \mathrm{d}V, \qquad (1.3)$$

where $j_{\mathrm{H}\beta}(T_e)$ is the emission coefficient of $\mathrm{H}\beta$ and is roughly proportional to $\alpha_B(\mathrm{H})$. Therefore the total luminosity in $\mathrm{H}\beta$ in an ionization bounded nebula is a direct measure of $Q(\mathrm{H}^0)$. At $T_e = 10^4$ K, it is given by:

$$L_{\rm H\beta} = 4.8 \ 10^{-13} Q({\rm H}^0) {\rm erg \ s}^{-1}.$$
(1.4)

In the case of a density bounded nebula, though, some ionizing photons escape and $L_{(H\beta)}$ is then given by:

$$L_{\rm H\beta} = 1.5 \ 10^{32} (T_e/10^4)^{-0.9} M_{neb} < n > \rm erg \ s^{-1},$$
(1.5)

where M_{neb} is the nebular mass in solar units and $\langle n \rangle$ is defined as:

$$\langle n \rangle = \int n^2 \epsilon \mathrm{d}V / \int n \epsilon \mathrm{d}V,$$
 (1.6)

assuming that in the nebula $n(\mathbf{H}^+) = n_e = n(\mathbf{H}) \equiv n$.

Thus, in the density bounded case, the total H β luminosity does not say anything about $Q(\mathrm{H}^0)$, except that $Q(\mathrm{H}^0)$ has to be larger than the value required to obtain the observed luminosity in H β . For a given total nebular mass, $L_{\mathrm{H}\beta}$ is larger for denser nebulae, since recombinations are then more frequent.

For nebulae composed of pure hydrogen, the maximum ionizable mass of gas for a given value of $Q(\mathrm{H}^0)$ is, at $T_e = 10^4$ K:

$$M_{ion} = 3.210^{-45} Q(\mathrm{H}^0) / < n > \mathrm{M}_{\odot}.$$
 (1.7)

The following table gives the values of M_{ion} for a typical PN, an H II region ionized by an O7 star, and a giant H II region ionized by a cluster of stars representing a total mass of $10^4 \, M_{\odot}$ (a Salpeter mass function is assumed and the star masses range between 1 and 100 $\, M_{\odot}$).

The surface brightness of an object is an important parameter from the observational point of view. Indeed, for extended objects, it determines the detectability or the quality of the spectra. For illustrative purposes, let us consider here the simple case of an

	$Q(\mathrm{H}^0)$	M_{\star}	$M_{ m ion}$	$M_{ m ion}$
			$n=10^2~{\rm cm}^{-3}$	$n=10^4~{\rm cm}^{-3}$
planetary nebula single star H II region giant H II region	$\begin{array}{c} 310^{47} \ \mathrm{ph} \ \mathrm{s}^{-1} \\ 310^{48} \ \mathrm{ph} \ \mathrm{s}^{-1} \\ 310^{50} \ \mathrm{ph} \ \mathrm{s}^{-1} \end{array}$	$30 {\rm ~M_{\odot}}$		$\begin{array}{c} 10^{-1} \ {\rm M}_{\odot} \\ 1 \ {\rm M}_{\odot} \\ 10^{2} \ {\rm M}_{\odot} \end{array}$

TABLE 1. Typical masses of the ionizing stars (or star clusters) and maximum nebular ionizable masses

homogeneous sphere and define:

$$S_{\rm H\beta} = F_{\rm H\beta} / (\pi \theta^2) = L_{\rm H\beta} / (4\pi^2 R_{neb}^2),$$
 (1.8)

where $F_{H\beta}$ is the observed H β flux, θ is the angular radius of the nebula and R_{neb} its physical radius. With the help of the previous equations one obtains for the ionization bounded case:

$$S_{\rm H\beta} \propto (Q({\rm H}^0) n^4 \epsilon^2)^{1/3}$$
 (1.9)

and for the density bounded case:

$$S_{\rm H\beta} \propto (M_{\rm neb} n^5 \epsilon^2)^{1/3}.$$
 (1.10)

Thus better data will be obtainable for objects of higher densities, and objects with higher M_{neb} or $Q(\mathrm{H}^0)$.

The number fractions of He and heavy elements $(C, N, O...)^{\dagger}$ in real nebulae are about 10% and 0.1% respectively. Helium, although ten times less abundant than hydrogen, is the dominant source of absorption of photons at energies above 24.4 eV. For order of magnitudes estimates, however, the formulae given above can still be used, since each recombination of He roughly produces one photon that can subsequently be absorbed only by hydrogen. The same remark generally holds for photons above 54.4 eV in the spectra of PNe with hot nuclei (see however Stasińska & Tylenda 1986). Naturally, for detailed studies, a photoionization modelling is necessary that takes into account properly the transfer of the photons arising from the recombination to He⁰ and He⁺.

1.1.2. The ionization structure

At a distance r from the ionizing source, the number densities $n(X_i^j)$ and $n(X_i^{j+1})$ of the ions X_i^j and X_i^{j+1} are schematically related by the following expression:

$$n(\mathbf{X}_{i}^{j})Q(\mathbf{H}^{0})/r^{2}K = n(\mathbf{X}_{i}^{j+1})n_{e}\alpha(\mathbf{X}^{j}), \qquad (1.11)$$

where K is a factor taking into account the frequency distribution of the ionizing radiation field and the absorption cross section (note that, for simplicity, the charge exchange process is not included in this equation). Of course, ions X_i^{j+1} can exist only if the radiation field contains photons able to produce these ions, and the ratio $n(X_i^{j+1})/n(X_i^j)$ will be higher for higher effective temperatures of the ionizing source.

Integrating Eq. (1.11) over the nebular volume and using Eq. (1.2), it can be shown that, for a spherical nebula of constant density and filling factor and with an ionizing radiation of given effective temperature, the average ionic ratios are proportional to

† It is a tradition in nebular studies, to refer to elements other than H and He as "heavy elements" or "metals".

 $(Q(\mathrm{H}^0)n\epsilon^2)^{1/3}$. In other words, a nebula of density $n = 10^4 \,\mathrm{cm}^{-3}$ ionized by one star with $T_{\star} = 50\,000$ K will have the same ionization structure as a nebula of density $n = 10^2 \,\mathrm{cm}^{-3}$ ionized by one hundred such stars.

The ionization parameter is usually defined by

$$U = Q(\mathrm{H}^0) / (4\pi R^2 nc), \qquad (1.12)$$

where R is either the Strömgren radius, or a typical distance from the gas cloud to the ionizing star, and c is the speed of light. U is thus directly proportional to $(Q(\mathrm{H}^0)n\epsilon^2)^{1/3}$ in the case of a constant density sphere and this parameter describes the ionization structure.

It is important to be aware that equation (1.12) shows that at a given distance from the source, ionization drops when the density is increased locally (like in the case of a density clump). On the other hand, of two nebulae with uniform density and ionized by the same star, the highest average ionization will occur for the densest one.

The presence of intense lines of low ionized species such as [N II] $\lambda 6584$, [S II] $\lambda 6716$, $\lambda 6731$, [O I] $\lambda 6300$, is often considered in the literature as a signature of the presence of shocks. Shock models indeed predict that these lines are strong, but it must be kept in mind that pure photoionization models can also produce strong low ionization lines. This is for example the case for nebulae containing regions of low ionization due to gas compression (e.g. Dopita 1997 Stasińska & Schaerer 1999). Another example is that of nebulae excited by very high energy photons, for which the absorption cross-section is small and which induce a warm, only partially ionized zone.

1.2. Heating and cooling

During the photoionization process, the absorption of a photon creates a free electron which rapidly shares its energy with the other electrons present in the gas by elastic collisions, and thus heats the gas. The energy gains are usually dominated by photoionization of hydrogen atoms, although photoionization of helium contributes significantly. Intuition might suggest that T_e will decrease away from the ionizing source, since the ionizing radiation field decreases because of geometrical dilution and absorption in the intervening layers. This is actually not the case. The total energy gains per unit volume and unit time at a distance r from the ionizing source are schematically given by:

$$G = n(\mathrm{H}^{0}) \int_{h\nu_{0}}^{\infty} (4\pi J_{\nu}(r)/h\nu), a_{\nu}(\mathrm{H}^{0})(h\nu - h\nu_{0})\mathrm{d}h\nu$$
(1.13)

where

$$4\pi J_{\nu}(r) = \pi F_{\nu}(r) = \pi F_{\nu}(0) (R_{\star})^2 / r^2 \mathrm{e}^{-\tau_{\nu}(\mathbf{r})}.$$
 (1.14)

If ionization equilibrium is achieved in each point of the nebula, one has (in the "on-thespot case")

$$n(\mathbf{H}^{0}) \int_{h\nu_{0}}^{\infty} (4\pi J_{\nu}(r)/h\nu) a_{\nu}(\mathbf{H}^{0}) dh\nu = n(\mathbf{H}^{+}) n_{e} \alpha_{B}(\mathbf{H}).$$
(1.15)

Therefore, G can be written

$$G = n(\mathrm{H}^+) n_e \alpha_B(\mathrm{H}) < E >, \qquad (1.16)$$

where

$$\langle E \rangle = \int_{h\nu_0}^{\infty} (4\pi J_{\nu}(r)/h\nu) a_{\nu}(\mathbf{H}^0)(h\nu - h\nu_0) \mathrm{d}h\nu / \int_{h\nu_0}^{\infty} (4\pi J_{\nu}(r)/h\nu) a_{\nu}(\mathbf{H}^0) \mathrm{d}h\nu.$$
(1.17)

Thus $\langle E \rangle$ can be seen as the average energy gained per photoionization, and is roughly independent of r. It can be shown (see e.g. Osterbrock 1989), that when the ionization

source is a blackbody of temperature T_{\star} , one has $\langle E \rangle \approx (3/2)kT_{\star}$. Therefore:

G

$$\propto n^2 T_\star T_e^{-1},\tag{1.18}$$

meaning that the energy gains are roughly proportional to the temperature of the ionizing stars.

Thermal losses in nebulae occur through recombination, free-free radiation and emission of collisionally excited lines. The dominant process is usually due to collisional excitation of ions from heavy elements (with O giving the largest contribution, followed by C, N, Ne and S). Indeed, these ions have low-lying energy levels which can easily be reached at nebular temperatures. The excitation potentials of hydrogen lines are much higher, so that collisional excitation of H^0 can become important only at high electron temperatures.

For the transition l of ion j of an element X^i , in a simple two-level approach and when each excitation is followed by a radiative deexcitation, the cooling rate can be schematically written as

$$L_{coll}^{ijl} = n_e n(X_i^j) q_{ijl} h \nu_{ijl} = 8.63 \, 10^{-6} n_e n(X_i^j) \Omega_{ijl} / \omega_{ijl} T_e^{-0.5} \mathrm{e}^{(\chi_{ijl}/kT_e)} h \nu_{ijl}, \qquad (1.19)$$

where Ω_{ijl} is the collision strength, ω_{ijl} is the statistical weight of the upper level, and χ_{ijl} is the excitation energy.

If the density is sufficiently high, some collisional deexcitation may occur and cooling is reduced. In the two-level approach one has:

$$L_{coll}^{ijl} = n_e n(X_i^j) n_e q_{ijl} h \nu_{ijl} (1/(1 + n_e(q_{12} + q_{21})/A_{21})).$$
(1.20)

So, in a first approximation, one can write that the electron temperature is determined by

$$G = L = \sum_{ijl} L_{coll}^{ijl}, \tag{1.21}$$

where G is given by Eq. (1.18) and L_{coll}^{ijl} by Eq. (1.20).

The following properties of the electron temperature are a consequence of the above equations:

- T_e is expected to be usually rather uniform in nebulae, its variations are mostly determined by the mean energy of the absorbed stellar photons, and by the populations of the main cooling ions. It is only at high metallicities (over solar) that large T_e gradients are expected: then cooling in the O⁺⁺ zone is dominated by collisional excitation of fine structure lines in the ground level of O⁺⁺, while the absence of fine structure lines in the ground level of O⁺ forces the temperature to rise in the outer zones (Stasińska 1980a, Garnett 1992).

- For a given T_{\star} , T_e is generally lower at higher metallicity.

– For a given metallicity, T_e is generally lower for lower T_{\star} .

– For a given T_{\star} and given metallicity, T_e increases with density in regions where n is larger than a critical density for collisional deexcitation of the most important cooling lines (around 5 $10^2 - 10^3$ cm⁻³).

1.3. Line intensities

In conditions prevailing in PNe and H II regions the observed emission lines are optically thin, except for resonance lines such as H Ly α , C IV λ 1550, N V λ 1240, Mg II λ 2800, Si IV λ 1400, and some helium lines. Also the fine structure IR lines could be optically thick in compact H II regions or giant H II regions (however, the velocity fields are generally such that this is not the case). The fact that most of the lines used for abundance determinations are optically thin makes their use robust and powerful.

6

The intensity ratios of recombination lines are almost independent of temperature. On the other hand, intensity ratios of optical and ultraviolet collisional lines are strongly dependent on electron temperature if the excitation levels differ.

Abundances of metals with respect to hydrogen are mostly derived using the intensity ratio of collisionally excited lines with H β . It is instructive to understand the dependence of such emission line ratios with metallicity. Let us consider the [O III] λ 5007/H β line ratio and follow its behaviour as n(O)/n(H) decreases (from now on the notation n(O)/n(H) will be replaced by O/H). The temperature dependence of the [O III] λ 5007 and H β lines implies that:

$$[O III] \lambda 5007/H\beta \propto n(O)/n(H) T_e^{0.5} e^{-28764/T_e}.$$
 (1.22)

– At high metallicity (O/H around 10^{-3} and above), cooling is efficient and T_e is low. Energy is mainly evacuated by the [O III] $\lambda 88 \,\mu$ m line, whose excitation potential is 164 K. The cooling rate is then approximately given by

$$L = n(\mathcal{O}^{++})n_e T_e^{-0.5} \mathrm{e}^{164/T_e}.$$
 (1.23)

Eq. (1.21) implies that

$$[O III] \lambda 5007/H\beta \propto T_* e^{-(28764+164)/T_e}.$$
(1.24)

Since T_e increases with decreasing O/H, Eq. (1.24) shows that [O III] λ 5007/H β increases. Note the value of [O III] λ 5007/H β depends on T_{\star} , being larger for higher effective temperatures.

– At intermediate metallicities, (O/H of the order of $10^{-3} - 210^{-4}$), cooling is still mainly due to the oxygen lines, but the abundance of O/H being only moderate, T_e is higher, allowing collisional excitation of the [O III] λ 5007 line, which now becomes the dominant coolant. The cooling can then be roughly expressed by:

$$L = n(\mathcal{O}^{++})n_e T_e^{-0.5} \mathrm{e}^{-28764/T_e}.$$
 (1.25)

Eqs. (1.21) and (1.22) imply:

$$[O III] \lambda 5007/H\beta \propto T_{\star}, \qquad (1.26)$$

i.e. [O III] $\lambda 5007/\text{H}\beta$ is proportional to T_{\star} and independent of O/H.

– Finally, at low metallicity, when cooling is dominated by recombination and collisional excitation of hydrogen, T_e becomes independent of O/H. From Eq. (1.22), it follows that [O III] λ 5007/H β is proportional to O/H. It also depends on T_{\star} and on the average population of neutral hydrogen inside the nebula.

2. Basics of abundance determinations in ionized nebulae

2.1. Empirical methods

These are methods in which no check is made for the consistency of the derived abundances with the observed properties of the nebulae. They can be schematically subdivided into direct methods and statistical methods.

2.1.1. Direct methods

The abundance ratio of two ions is obtained from the observed intensity ratio of lines emitted by these ions. For example, O^{++}/H^+ can be derived from

$$O^{++}/H^{+} = \frac{[O \text{ III}] \lambda 5007/H\beta}{j_{[O \text{ III}](T_{e},n)}/j_{H\beta(T_{e})}},$$
(2.27)

where $j_{[O III]}(T_e, n)$ is the emission coefficient of the [O III] λ 5007 line, which is dependent on T_e and n (assumed uniform in the nebula).

 T_e can be derived using the ratio of the two lines [O III] λ 4363 and [O III] λ 5007, which have very different excitation potentials. Other line ratios can also be used as temperature indicators in nebulae, such as [N II] λ 5755/6584 and [S III] λ 6312/9532. The Balmer and Paschen jumps, the radio continuum and radio recombination lines also allow to estimate the electron temperature, but the measurements are more difficult.

The density is usually derived from intensity ratios of two lines of the same ion which have the same excitation energy but different collisional deexcitation rates. The most common such ratio is [S II] $\lambda 6731/6717$. Far infrared lines can also be used to determine densities. Each line pair is sensitive in a given density range (about 2 to 3 decades), which can be ranked as follows (Rubin *et al.* 1994): [N II] $\lambda 122\mu/205\mu$, [O III] $\lambda 52\mu/88\mu$, [S II] $\lambda 6731/6717$, [O II] $\lambda 3726/3729$, [S III] $\lambda 18.7\mu/33.6\mu$, [A IV] $\lambda 4740/4711$, [N III] $\lambda 15.5\mu/36.0\mu$, [A III] $\lambda 8.99\mu/21.8\mu$, C III] $\lambda 1909/1907$. The electron density can also be measured by the ratio of high order hydrogen recombination lines.

Plasma diagnostic diagrams combining all the information from temperature- and density-sensitive line ratios can also be constructed for a given nebula (e.g. Aller & Czyzak 1983), plotting for each pair of diagnostic lines the curve in the (T_e, n) plane that corresponds to the observed value. The curves usually do not intersect in one point, due to measurement errors and to the fact that the nebula is not homogeneous (and also to possible uncertainties in the atomic data) and provide a visual estimate of the uncertainty in the adopted values of T_e and n.

The total abundance of a given element relative to hydrogen is given by the sum of abundances of all its ions. In practise, not all the ions present in a nebula are generally observed. The only favourable case is that of oxygen which in H II regions is readily determined from:

$$O/H = O^{+}/H^{+} + O^{++}/H^{+}.$$
 (2.28)

Note that even if $[O I] \lambda 6300$ is observed, it should not be included in the determination of the oxygen abundance, since the reference hydrogen line is emitted by H⁺, while O⁰ is tied to H⁰.

In almost all other cases (except in some cases when multiwavelength data are available), one must correct for unseen ions using ionization correction factors. A common way to do this in the 70' and 80' and even later was to rely on ionization potential considerations, which led to such simple expressions as:

$$N/O = N^+/O^+,$$
 (2.29)

$$Ne/O = Ne^{++}/O^{++},$$
 (2.30)

$$C/O = C^{++}/O^{++}.$$
 (2.31)

In high excitation PNe where He II lines are seen, oxygen can be present in ionization stages higher than O^{++} . A popular ionization correction scheme for oxygen (e.g. Torres-Peimbert & Peimbert 1977) was:

$$\frac{O}{H} = \frac{(He^+ + He^{++})}{He^+} \frac{(O^+ + O^{++})}{H^+}.$$
(2.32)

Expressions (2.29 - 2.31) are based on the similarity the ionization potentials of C⁺, N⁺, O⁺, Ne⁺. Expression (2.32) is based on the fact that the ionization potentials of He⁺ and O⁺⁺ are identical.

However, photoionization models show that such simple relations do not necessarily hold. For example, the charge transfer reaction $O^{++} + H^0 \rightarrow O^+ + H^+$ being much more efficient than the Ne⁺⁺ + H⁰ \rightarrow Ne⁺ + H⁺ one, Ne⁺⁺ is more recombined than O^{++} in the outer parts of nebulae and in zones of low ionization parameter.

8

Also, while it is true that no O^{+++} ions can be found outside the He⁺⁺ Strömgren sphere, since the photons able to ionize O^{++} are absorbed by He⁺, O^{++} ions can well be present inside the He⁺⁺ zone.

Ionization correction factors based on grids of photoionization models of nebulae are therefore more reliable. Complete sets of ionization correction factors have been published by Mathis & Rosa (1991) for H II regions and Kingsburgh & Barlow (1994) for planetary nebulae, or can be computed from grid of photoionization models such as those of Stasińska (1990), Gruenwald & Viegas (1992) for single star H II regions, Stasińska et al. (2001) for giant H II regions, Stasińska et al. (1998) for PNe.

However, it must be kept in mind that ionization correction factors from model grids may be risky too, both because the atomic physics is not well known yet (see Sect. 3.1) and because the density structure of real nebulae is more complicated than that of idealized models. The most robust relation seems to be $N/O = N^+/O^+$ (but see Stasińska & Schaerer 1997). Such a circumstance is fortunate, given the importance of the N/O ratio both in H II regions (as a constraint for chemical evolution studies) and in PNe (as a clue on PNe progenitors).

In spite of uncertainties, ionization correction factors often provide more accurate abundances than summing up ionic abundances obtained combining different techniques in the optical, ultraviolet and infrared domains.

Note that there is no robust empirical way to correct for neutral helium to derive the total helium abundance. The reason is that the relative populations of helium and hydrogen ions mostly depend on the energy distribution of the ionizing radiation field, while those of ions from heavy elements are also a function of the gas density distribution.

In summary, direct methods for abundance determinations are simple, powerful, and provide reasonable results (provided one keeps in mind the uncertainties involved, which will be developed in the next sections). Until recently, abundances were mostly derived from collisionally excited optical lines. This is still the case, but the importance of infrared data is growing, especially since the ISO mission. IR line intensities have the advantage of being almost independent of temperature. They arise from a larger variety of ions than optical lines. They allow to probe regions highly obscured by dust. However, they suffer from beamsize and calibration problems which are far more difficult to overcome than in the case of optical spectra. Abundance determinations using recombination lines of heavy elements have regained interest these last years. They require high signal-to-noise spectroscopy since the strengths of recombination lines from heavy elements are typically 0.1% of those of hydrogen Balmer lines. They will be discussed more thoroughly in the next sections, since they unexpectedly pose one of the major problems in nebular astrophysics.

2.1.2. Strong line or statistical methods

When the electron temperature cannot be determined, for example because the observations do not cover the appropriate spectral range or because temperature sensitive lines such as [O III] λ 4363 cannot be observed, one has to go for statistical methods or "strong line methods". These methods have first been introduced by Pagel et al. (1979) to derive metallicities in giant extragalactic H II regions. They have since then being reconsidered and recalibrated by many authors, among which Skillman (1989), McGaugh (1991, 1994), Pilyugin (2000, 2001).

Pagel et al. (1979) proposed to use the 4 strongest lines of O and H : H α , H β , [O II] λ 3727 and [O III] λ 5007. From Sect. 1, the main parameters governing the relative intensities of the emission lines in a nebula are : $\langle T_{\star} \rangle$, the mean effective temperature of the ionization source, the gas density distribution (parametrized by U in the case of

10

homogeneous spheres), and the metallicity, represented by O/H. Luckily oxygen is at the same time the main coolant in nebulae, and the element whose abundance is most straightforwardly related to the chemical evolution of galaxies. The spectra must be corrected for reddening, which is done by comparing the observed $H\alpha/H\beta$ ratio with the case B recombination value at a typical T_e and assuming a reddening law (see Sect. 3.3). Therefore two independent line ratios, [O II] $\lambda 3727/H\beta$ and [O III] $\lambda 5007/H\beta$, remain to determine three quantities. Statistical methods rely on the assumption that $\langle T_{\star} \rangle$ (and possibly U) are closely linked to the metallicity, and that it is the metallicity which drives the observed line ratios. Basing on available photoionization model grids, Pagel et al. showed that ([O II] $\lambda 3727 + [O III] \lambda 5007$)/H β , later called O₂₃, could be used as an indicator of O/H at metallicities above half-solar. Skillman (1989) later argued that this ratio could also be used in the low metallicity regime, in cases when the observations did not have sufficient signal-to-noise to measure the [O III] λ 4363 line intensity. McGaugh (1994) improved the method and proposed to use both [O III] $\lambda 5007/[O II] \lambda 3727$ and O_{23} to determine simultaneously O/H and U (his method should perhaps be called the O_{23+} method). For the reasons explained above, the same value of ([O II] $\lambda 3727$ + $[O \text{ III}] \lambda 5007)/\text{H}\beta$ can correspond to either a high or a low value of the metallicity. A useful discriminator is [N II] $\lambda 6584/[O II] \lambda 3727$, since it is an empirical fact that [N II] $\lambda 6584/[O \text{ II}] \lambda 3727$ increases with O/H (McGaugh 1994).

The expected accuracy of statistical methods is typically 0.2 - 0.3 dex, the method being particularly insensitive in the turnover region at O/H around 3 10^{-4} .

On the low metallicity side, the method can easily be calibrated with data on metalpoor extragalactic H II regions where the [O III] λ 4363 line can be measured. Recently, Pilvugin (2000) has done this using the large set of excellent quality observations of blue compact galaxies by Izotov and coworkers (actually, the strong line method proposed by Pilyugin differs somewhat from the O_{23} method, but it relies on similar principles). He showed that the method works extremely well at low metallicities (with an accuracy of about 0.04 dex). This is a priori surprising, since giant H II regions are powered by clusters of stars that were formed almost coevally. The most massive stars die gradually, inducing a softening of the ionizing radiation field on timescales of several Myr, which should affect the O_{23} ratio, as shown by McGaugh (1991) or Stasińska (1998). As discussed by Stasińska et al. (2001), data on H II regions in blue compact dwarf galaxies are probably biased towards the most recent starbursts, and the dispersion in $\langle T_{\star} \rangle$ is not as large as could be expected a priori. Another possibility, advocated by Bresolin et al. (1999) in their study of giant H II regions in spiral galaxies is that some mechanism must disrupt the H II regions after a few Myr. Of course, the O_{23} method is expected of much lower accuracy when applied to H II regions ionized by only a few stars, since in that case the ionizing radiation field varies strongly from object to object.

On the high metallicity side (O/H larger than about 5 10^{-4}), the situation is much more complex. In this regime, there is so far no direct determination of O/H to allow a calibration of the O₂₃ method since the [O III] λ 4363 line is too weak to be measured (at least with 4 m class telescopes). The calibrations rely purely on models but it is not known how well these models represent real H II regions. Besides, at these abundances, the [O II] λ 3727 and [O III] λ 5007 line intensities are extremely sensitive to any change in the nebular properties (Oey & Kennicutt 1993, Henry 1993, Shields & Kennicutt 1995). Note that the calibration proposed by Pilyugin (2001) of his related X₂₃ method in the high metallicity regime actually refers to O/H ratios that are lower than 5 10^{-4} .

Other methods have been proposed as substitutes to the O_{23} method. The S_{23} method, proposed by Vílchez & Esteban (1996) and Díaz & Pérez-Montero (2000) relies on the same principles as the O_{23} method, but uses ([S II] $\lambda 6716$, $\lambda 6731 + [S III] \lambda 9069$, λ 9532)/H β (S₂₃) instead of ([O II] λ 3727 + [O III] λ 5007)/H β . One advantage over the O₂₃ method is that the relevant line ratios are less affected by reddening. Besides, the excitation levels of the [S II] λ 6716, λ 6731 and [S III] λ 9532 lines are lower than those of the [O II] λ 3727 and [O III] λ 5007 lines, so that S₂₃ increases with metallicity in a wider range of metallicities than O₂₃ (the turnover region for S₂₃ is expected at O/H around 10⁻³). Unfortunately, [S III] λ 9532 is more difficult to observe than [O III] λ 5007. Oey & Shields (2000) argue that the S₂₃ method is more sensitive to U than claimed by Diaz & Perez-Montero (2000). This would require futher checks, but in any case, the S₂₃ method could be refined into an S₂₃₊ method in the same way as the O₂₃ was refined into the O₂₃₊ method.

Stevenson et al. (1993) proposed to use [Ar III] λ 7136] / [S III] λ 9532 as an indicator of the electron temperature in metal-rich H II regions, and therefore of their metallicity. This method relies on the idea that the Ar/S ratio is not expected to vary significantly from object to object, and that the Ar⁺⁺ and S⁺⁺ zones should be coextensive. However, photoionization models show that, because of the strong temperature gradients expected at high metallicity, this method could lead to spurious results.

Alloin et al. (1979) proposed to use [O III] λ 5007/[N II] λ 6584 as a statistical metallicity indicator. While this line ratio depends on an additional parameter, namely N/O, the accuracy of this method turns out to be similar to that of statistical methods mentioned above. More recently, Storchi-Bergman et al. (1994), van Zee et al. (1998) and Denicolo et al. (2001) advocated for the use of the [N II] λ 6584/H β ratio (N₂) as metallicity indicator. Similarly to [N II] λ 6584/[O III] λ 5007, this ratio shows to be correlated with O/H over the entire range of observed metallicities in giant H II regions. The reason why, contrary to the O₂₃ ratio, it increases with O/H even at high metallicity is due to a conjunction of [N II] λ 6584/H β being less dependent on T_e than O₂₃, N/O being observed to increase with O/H in giant H II regions (at high metallicity at least) and U tending to decrease with metallicity. The advantage of this ratio is that it is independent of reddening and of flux calibration, and is only weakly affected by underlying stellar absorption in the case of observations encompassing old stellar populations. This makes it extremely valuable for ranking metallicities of galaxies up to redshifts about 2.5.

As mentioned above, statistical methods for abundance determinations assume that the nebulae under study form a one parameter family. This is why they work reasonably well in giant H II regions. They are not expected to work in planetary nebulae, where the effective temperatures range between 20000 K and 200000 K. Still, it has been shown empirically that there is an upper envelope in the [O III] λ 5007/H β vs. O/H relation (Richer 1993), probably corresponding to PNe with the hottest central stars. The existence of such an envelope can be used to obtain lower limits of O/H in PNe located in distant galaxies.

2.2. Model fitting

2.2.1. Philosophy of model fitting

A widely spread opinion is that photoionization model fitting provides the most accurate abundances. This would be true if the constraints were sufficiently numerous (not only on emission line ratios, but also on the stellar content and on the nebular gas distribution) and if the model fit were perfect (with a photoionization code treating correctly all the relevant physical processes and using accurate atomic data). These conditions are never met in practise, and it is therefore worth thinking, before embarking on a detailed photoionization modelling, what is the aim one is pursueing.

Two opposite situations may arise when trying to fit observations with a model.

The first one occurs when the number of strong constraints is not sufficient, especially

when no direct T_e indicator is available. Then various models may be equally well compatible with the observations. For example, from a photoionization model analysis Ratag et al. (1997) derive an O/H ratio of 2.2 10^{-4} for the PN M 2-5. However, if one explores the range of acceptable photoionization models one finds two families of solutions (see Stasińska 2002). The first has O/H $\simeq 2.4 \ 10^{-4}$, the second has O/H $\simeq 1.2 \ 10^{-3}$! The reason for such a double solution is simply the behaviour of [O III] $\lambda 5007/\text{H}\beta$ or [O II] $\lambda 3727/\text{H}\beta$ with metallicity, as explained in Sect. 1.3. Note that both families of models reproduce not only the observed line ratios (including upper limits on unobserved lines) but also the nebular size and total H β flux.

The other situation is when, on the contrary, one cannot find any solution that reproduces at the same time the [O III] λ 4363/5007 line ratio and the constraints of the distribution of the gas and ionizing star(s) (e.g. Peña et al. 1998, Luridiana et al. 1999, Stasińska & Schaerer 1999). The model that best reproduces the strong oxygen lines has a different value of O/H than would be derived using an empirical electron-temperature based method. The difference between the two can amount to factors as large as 2 (Luridiana et al. 1999). It is difficult to say a priori which of the two values of O/H – if any – is the correct one.

The situation where the number of strong constraints is large and everything is satisfactorily fitted with a photoionization model is extremely rare. One such example is the case of the two PNe in the Sgr B2 galaxy, for which high signal-to-noise integrated spectra are available providing several electron temperature and density indicators with accuracy of a few %. Dudziak et al. (2000) reproduced the 33 (resp. 27) independent observables (including imagery and photometry) with two-density component models having 18 (resp. 14) free parameters for Wray 16-423 (resp. He 2-436). Still, the models are not really unique. The authors make the point that they can reproduce the present observations with a range of values for C/H and T_{\star} . Yet, the derived abundances are not significantly different from those obtained from the same observational data by Walsh et al. (1997) using the empirical method. The only notable difference is for sulfur whose abundance from the models is larger by 50%, and for nitrogen whose abundance from the models is larger by a factor of 2.8 in the case of He 2-436. This apparent discrepancy for the nitrogen abundance actually disappears if realistic error bars are considered for the direct abundance determinations (rather than the error bars quoted in the papers). Indeed, the fact that the nebular gas is rather dense, with different density indicators pointing at densities from $3 \ 10^3 \ \mathrm{cm}^{-3}$ up to over $10^5 \ \mathrm{cm}^{-3}$ introduces important uncertainties in the temperature derived from [N II] $\lambda 5755/6584$ due to collisional deexcitation. It must be noted that realistic error bars on abundances derived from model fitting are extremely difficult to obtain, since this would imply the construction of a tremendous number of models, all fitting the data within the observational errors.

To summarize, abundances are not necessarily better determined from model fitting. However, model fitting, if done with a sufficient number of constraints, provides ionization correction factors relevant for the object under study that should be more accurate than simple formulae derived from grids of photoionization models. This could be called a "hybrid method" to derive abundances. Such a method was for example used by Aller & Czyzak (1983) and Aller & Keyes (1987) to derive the abundances in a large sample of Galactic planetary nebulae, and is still being used by Aller and his coworkers. It must however be kept in mind that if photoionization models do not reproduce the temperature sensitive line ratios, this actually points to a problem that has to be solved before one can claim to have obtained reliable abundances.

Ab initio photoionization models are sometimes used to estimate uncertainties that can be expected in abundance determinations from empirical methods. For example Alexander & Balick (1997) and Gruenwald & Viegas (1998) explored the validity of traditional ionization correction factors in the case of spatially resolved observations. A complete discussion of uncertainties should also take into account uncertainties in the atomic data and the effect of a simplified representation of reality by photoionization models.

2.2.2. Photoionization codes

Photoionization codes are built to take into account all the major physical processes that govern the ionization and temperature structure of nebulae. In addition to photoionization, recombination, free-free radiation, collisional excitation they consider collisional ionization (this is important only in regions of coronal temperatures), charge exchange reactions, which are actually a non negligible cause of recombination for heavy elements, especially if the physical conditions are such that the population of residual hydrogen atoms in the ionized gas exceeds 10^{-3} . Some codes are designed to study nebulae that are not in equilibrium and they may include such processes as mechanical heating and expansion cooling.

Most nebular studies use static photoionization codes, which assume that the gas is in ionization and thermal equilibrium. The most popular one is CLOUDY developed by Ferland and co-workers, for which an extensive documentation is available and which is widely in use (see Ferland 1998, and http://www.pa.uky.edu/~gary/cloudy/ for the latest release). Several dozens of independent photoionization codes suited for the study of PNe and H II regions have been constructed over the years. Some of them have been intercompared at several workshops (Péquignot 1986, Ferland et al. 1996 and Ferland & Savin 2001). The codes mainly differ in the numerical treatment of the transfer of the ionizing photons produced in the nebula: on the spot reabsorption, outward-only approximation (most codes presently), full treatment (either with classical techniques as in Rubin 1968 or Harrington 1968 or with Monte-Carlo techniques as in Och et al. 1998). They also differ in their capacity of handling different geometries. Most codes are built in plane parallel or spherical approximations, but a few are built in 3D (Gruenwald et al. 1997, Och et al. 1998). While 3D codes are better suited to represent the density distribution in real nebulae, their use is hampered by the fact that the number of free parameters is extremely large. Presently, simpler codes are usually sufficient to pinpoint difficulties in fitting observed nebulae within our present knowledge of the physical processes occuring in them and to settle error bars on abundance determinations.

When the timescale of stellar evolution becomes comparable to the timescale of recombination processes, the assumption of ionization equilibrium is no more valid. This for example occurs in PNe with massive ($>0.64 \text{ M}_{\odot}$) nuclei, whose temperature and luminosity drop in a few hundred years while they evolve towards the white dwarf stage. In that case, the real ionization state of the gas is higher than would be predicted by a static photoionization model, and a recombining halo can appear. To deal with such situations, one needs time dependent photoionization codes, such as those of Tylenda (1979), or Marten & Szczerba (1997).

The nebular gas is actually shaped by the dynamical effect of the stellar winds from the ionizing stars. This induces shocks that produce strong collisional heating at the ionization front or at the interface between the main nebular shell of swept-up gas and the hot stellar wind bubble. On the other hand, expansion contributes to the cooling of the nebular gas. Several codes have been designed to treat simultaneously the hydrodynamical equations and the microphysical processes either in 1D (e.g. Schmidt-Voigt & Köppen 1987a and b, Marten & Schönberner 1991, Frank & Mellema 1994a, Rodriguez-Gaspar & Tenorio-Tagle 1998) or in 2D (Frank & Mellema 1994b, Mellema & Frank 1995,

Mellema 1995). It may be that some of the problems found with static codes will find their solution with a proper dynamical description. However, so far, for computational reasons, the microphysics and transfer of radiation is introduced in a more simplified way in these codes. Also, it is much more difficult to investigate a given problem with such codes, since the present state of an object is the result of its entire history, which has to be modelled ab initio.

3. Main problems and uncertainties in abundance determinations

The validity of derived abundances depends on the quality of the data and on the method of analysis. Typical quoted values for the uncertainties are 0.1 - 0.25 dex for ratios such as O/H, N/H, Ne/H, a little more for S/H, A/H, C/H, a little less for N/O, Ne/O and a few % for He. The optimism of the investigator is an important factor in the evaluation of the accuracy. This section comments on the various sources of uncertainties in abundance determinations.

3.1. Atomic data

Reviews on atomic data for abundance analysis have been given by Mendoza (1983), Butler (1993), Storey (1997), Nahar (2002). On-line atomic data bases are available from different sites. For example http://plasma-gate.weizmann.ac.il/DBfAPP.html provides links to many sites of interest, including the site of CLOUDY. The XSTAR atomic data base, constructed by Bautista & Kallman (2001) and used in the photoionization code XSTAR can be found at http://heasarc.gsfc.nasa.gov/docs/software/xstar/xstar.html.

The OPACITY and IRON projects (Seaton 1987, Hummer et al. 1993) have considerably increased the reliability of atomic data used for nebular analysis in the recent years. In the following, we simply raise a few important points.

3.1.1. Ionization, recombination and charge exchange

Until recently, photoionization cross sections and recombination (radiative and dielectronic) coefficient sets used in photoionization computations were not obtained selfconsistently. Photoionization and recombination calculations are presently being carried out using the same set of eigenfunctions as in the IRON project (Nahar & Pradhan 1997, Nahar et al. 2000). The expected overall uncertainty is 10 - 20%. Experimental checks on a few species (see e.g. Savin 1999) can provide benchmarks for confrontation with numerical computations.

Concerning charge exchange, only a few detailed computations are available (see references in the compilation by Kingdon & Ferland 1996). Coefficients computed with the Landau-Zeener approximation are available for most ions of interest. They are unfortunately rather uncertain. Differences with coefficients from quantal computations, which are available for a few species only, can be as large as a factor 3.

Due to the uncertainties in atomic parameters, the ionization structure predicted by photoionization models is so far expected to be accurate only for elements from the first and second row of the Mendeleev table.

3.1.2. Transition probabilities, collision strengths and effective recombination coefficients

The atomic data to compute the emissivities of optical forbidden lines have been recently recomputed in the frame of the IRON project (Hummer et al. 1993). The expected accuracies are typically of 10% for second row elements, however, the uncertainty is difficult to determine internally. Comparison with laboratory data is scarce, and actually, PNe are sometimes used as laboratories to test atomic physics calculations. For example,

van Hoof et al. (2000) studied 3 PNe in detail and concluded that the [Ne V] collision strenghts computed by Lennon & Burke (1994) should be correct within 30 %, contrary to previous suggestions by Oliva et al. (1996) and Clegg et al. (1987). Another example is the density derived from $[O III] \lambda 52 \,\mu m/[O III] \lambda 88 \,\mu m$, which is significantly lower than derived from [S II] $\lambda 6731/6717$ and [Ar IV] $\lambda 4711+4740$ for a large sample of PNe observed by ISO (Liu et al. 2001). These authors argue that [O III] IR lines can be emitted from rather low density components but it could just be that the atomic data are in error.

Concerning recombination lines, the effective recombination rates for lines from hydrogenic ions have been recomputed by Storey & Hummer (1995) and by Smits (1996) for He I λ 5876. For C, N, O, estimates for all important optical and UV transitions are given by Péquignot et al. (1991). Detailed computations of effective recombination coefficients are now available for lines from several ions of C, N, O and Ne (see e.g. a compilation in Liu et al. 2000). Note however that these do not include dielectronic recombination for states with high quantum number, which may have important consequences for the interpretation of recombination line data (see Sect. 3.6)

3.2. Stellar atmospheres

The ionization structure of nebulae obviously depends on the spectral distribution of the stellar radiation field. The theory of stellar atmospheres has made enormous progress these last years, due to advanced computing facilities. Several sets of models for massive O stars and for PNe nuclei are now available. The most detailed stellar atmosphere computations now include non-LTE effects and blanketing for numerous elements (e.g. Dreizler & Werner 1993, Hubeny & Lanz 1995, Rauch et al. 2000) and supersede previous works. The effect of winds, which is especially important for evolved stars such as Wolf-Rayet stars, is included in several codes, although with different assumptions (Schaerer & de Koter 1997, Hillier & Miller 1998, Koesterke et al. 2000, Pauldrach et al. 2001).

The resulting model atmospheres differ considerably between each other in the extreme UV. This has a strong impact on the predicted nebular ionization structure (see e.g. Stasińska & Schaerer 1997 for the Ne and the N^+/O^+ problems). Actually, the confrontation of photoionization models with observations of nebulae is expected to provide tests of the ionizing fluxes from model atmospheres (see Oey et al. 2000, Schaerer 2000, Giveon et al. 2002, Morisset et al. 2002). This is especially rewarding with the ISO data which provide accurate measurements for many fine-structure lines of adjacent ions.

For exploration purposes, it is sometimes sufficient to assume that the ionizing stars radiate as blackbodies, e.g. when interested in a general description of the temporal evolution of PNe spectra as their nuclei evolve from the AGB to the white dwarf stage (e.g. Schmidt Voigt & Köppen 1987a, b, Stasińska et al. 1998). On the other hand, for a detailed model analysis of specific objects, the black body approximation is generally not well suited. For example, the emission of [Ne v] lines in PNe cannot be understood when using blackbodies of reasonable temperatures.

3.3. Reddening correction

The usual dereddening procedure is to derive the logarithmic extinction at H β , C, from the observed H α /H β ratio, assuming that the intrinsic one has the value (H α /H β)_B predicted by case B recombination:

$$C = \left[\log(\mathrm{H}\alpha/\mathrm{H}\beta)_{\mathrm{B}} - \log(\mathrm{H}\alpha/\mathrm{H}\beta)_{obs}\right] / (f_{\alpha} - f_{\beta}), \qquad (3.33)$$

where f_{α} and f_{β} represent the values of the reddening law at the wavelengths of the H α and H β lines respectively.

16

Then, for any observed line ratio $(F_{\lambda 1}/F_{\lambda 2})_{obs}$ one can obtain the reddening corrected value $(F_{\lambda 1}/F_{\lambda 2})_{corr}$ from:

$$\log(F_{\lambda 1}/F_{\lambda 2})_{corr} = \log(F_{\lambda 1}/F_{\lambda 2})_{obs} + C(f_{\lambda 1} - f_{\lambda 2}).$$
(3.34)

Ideally, one can iterate after having determined the electron temperature of the plasma, to use a value of $(H\alpha/H\beta)_B$ at the appropriate temperature.

There are nevertheless several problems. One is that the extinction law is not universal. As shown by Cardelli et al. (1989), it depends on the parameter $R_V = A_V/E(B-V)$, where A_V is the absolute extinction in V and E(B-V) is the color excess. While the canonical value of R_V is 3–3.2, the actual values range from 2.5 to 5 (Cardelli et al. 1989, Barbaro et al. 2001, Patriarchi et al. 2001). Objects located in the Galactic bulge suffer from an extinction characterized by a low value of R_V (e.g. Stasińska et al. 1992, Liu et al. 2001). Cardelli et. el. (1989) attribute these differences in extinction laws between small and large values of R_V to the presence of systematically larger particles in dense regions. These variations in R_V have a significant effect on line ratios when dealing with ultraviolet spectra. It is therefore convenient to link the optical and ultraviolet spectra by using line ratios with known intrinsic value, such as He II $\lambda 1640$ / He II $\lambda 4686$.

Another difficulty is that dust is not necessarily entirely located between the object and the observer as in the case of stars. Some extinction may be due to dust mixed with the emitting gas. In that case, the wavelength dependence of the extinction is different and strongly geometry dependent (Mathis 1983). One way to proceed, which alleviates this problem, is to use the entire set of observed hydrogen lines and fit their ratios to the theoretical value, which then gives an empirical reddening law to deredden the other emission lines. This, however, is still not perfect, since the extinction suffered by lines emitted only at the periphery of the nebula, or, on the contrary, only in the central parts, is different from the extinction suffered by hydrogen lines which are emitted in the entire nebular body. The problem is further complicated by scattering effects (see e. g. Henney 1998).

In the case of giant H II regions, where the observing slit encompasses stellar light, one must first correct for the stellar absorption in the hydrogen lines. This can be done in an iterative procedure, as outlined for example by Izotov et al. (1994).

A further problem is that the intrinsic hydrogen line ratios may deviate from case B theory. This occurs for example in nebulae with high electron temperature (~ 20000 K), where collisional contribution to the emissivity of the lowest order Balmer lines may become significant. In that case, a line ratio corrected assuming case B for the hydrogen lines, $(F_{\lambda 1}/F_{\lambda 2})_{\rm B}$ is related to the true line ratio $(F_{\lambda 1}/F_{\lambda 2})_{true}$ by:

$$\log(F_{\lambda 1}/F_{\lambda 2})_{\rm B} - \log(F_{\lambda 1}/F_{\lambda 2})_{true} = \left[\log({\rm H}\alpha/{\rm H}\beta)_{\rm B} - \log({\rm H}\alpha/{\rm H}\beta)_{true}\right](f_{\lambda 1} - f_{\lambda 2})/(f_{\alpha} - f_{\beta}).$$
(3.35)

The error is *independent of the real extinction* and can be large for $\lambda 1$ very different from $\lambda 2$. For example, it can easily reach a factor 1.5 - 2 for C III] $\lambda 1909/[O III] \lambda 5007$ (see Stasińska 2002).

Whatever dereddening procedure is adopted, it is good practise to check whether the $H\gamma/H\beta$ value has the expected value. If not, the [O III] λ 4363/5007 ratio will be in error by a similar amount.

3.4. Aperture correction, nebular geometry and density inhomogeneities

Observations are made with apertures or slits that often have a smaller projected size on the sky than the objects under study. When combining data obtained with different instruments, one needs to correct for aperture effects. To merge spectra obtained by IUE with optical spectra, one can use pairs of lines of the same ion such as He II $\lambda 1640$ and

He II λ 4686. However, ionization stratification and reddening make the problem difficult to solve. One can also use C III] λ 1909 and C II λ 4267, but this involves additional difficulties (see Sect. 3.6). Summarizing, aperture corrections can be wrong by a factor as large as 2 (Kwitter & Henry 1998, van Hoof et al. 2000).

Interpretation of emission line ratios should care whether the observing slit covers the entire nebula, at least in the estimation of error bars on derived quantities. This is especially important when the observations cover only a small fraction of the total volume. Gruenwald & Viegas (1992) have published line of sight results for grids of H II region models, that can be used to estimate the ionization correction factors relevant to H II region spectra observed with small apertures. Alexander & Balick (1997) and Gruenwald & Viegas (1998) have considered the case of PNe, and shown that traditional ionization correction factors may strongly overestimate (or underestimate) the N/H ratio in the case when the slit size is much smaller than the apparent size of the nebula. The ratio N/O is less affected by line of sight effects. The problem is of course even worse in real nebulae than in those idealized models, due to the presence of small scale density variations. Integrated spectra have the merit on being less dependent on local conditions and of being more easily comparable to models. For extended nebulae, they can be obtained by scanning the slit across the face of the nebula (van Hoof et al. 2000, Liu et al. 2000), or by using specially designed nebular spectrophotometers (Caplan et al. 2000).

Tailored modelling taking explicitly into account departure from spherical symmetry is still in its infancy. One may mention the work of Monteiro et al. (2000) who constructed a 3D photoionization model to reproduce the narrow band HST images and velocity profiles of the PN NGC 3132 and concluded that this nebula has a diabolo shape despite its elliptical appearance. For the abundance determination however, which is the topic of this review, their finding has actually no real incidence.

More relevant for abundance determinations are the works of Sankrit & Hester (2000) and Moore et al. (2000), who modelled individual filaments in large nebulae, trying to reproduce the emission line profiles in several lines. Such a method uses many more constraints than classical T_e -based methods to derive abundances, but would need additional line ratios, and especially the T_e indicators, to be validated.

If large density contrasts occur in ionized nebulae, the use of forbidden lines for abundance determinations may induce some bias if collisional deexcitation is important. These biases have been explored by Rubin (1989) and his "maximum bias table" can be used to confine errors in abundances due to these effects.

3.5. Spatial temperature variations

3.5.1. Temperature gradients

At high metallicities, as explained above, large temperature gradients are expected in ionized nebulae. Therefore, empirical methods based on [O III] λ 4363/5007 will underestimate the abundances of heavy elements, since the [O III] λ 4363 line will be essentially emitted in the high temperature zones, inducing a strong overestimate of the average T_e . Therefore, although with very large telescopes it will now be possible to measure [O III] λ 4363 even in high metallicity giant H II regions, one should refrain from exploiting this line in the usual way. Doing this, one would necessarily find sub-solar oxygen abundances, even for giant H II regions with metallicities well above solar (Fig. 3 of Stasińska 2002). High metallicity *luminous* PNe offer a much safer way to probe the metallicity in central parts of galaxies (see Sect. 5.3 for the relevance of PNe as metallicity indicators of their environment). Indeed the higher effective temperatures and the higher densities in *luminous* PNe induce higher values of T_e in the O⁺⁺ zone and a shallower temperature

gradient, leading to a negligible bias in the derived abundances (see Fig. 4 of Stasińska 2002).

While T_e -based empirical methods are biased for metal rich giant H II regions, tailored photoionization modeling to reproduce the *distribution* of the emission in the H α , H β , He I λ 5876, [O II] λ 3727and [O III] λ 5007 lines are worth trying. As suggested by Stasińska (1980a), at high metallicity, regions emitting strongly [O III] λ 5007 will be decoupled from the regions emitting strongly in the recombination lines, and would be almost cospatial with regions emitting most of [O II] λ 3727. While the models of Stasińska (1980a) were made under spherical symmetry, the statement is more general, because it relies of the principles of ionization and thermal balance outlined in Sects. 1.1 and 1.2.

3.5.2. Small scale temperature variations

If the temperature in a nebula is not uniform, T_e -based empirical abundances are biased. Peimbert (1967) developed a mathematical formulation to evaluate the bias. It is based on the Taylor expansion of the average temperature

$$T_o(N_i) = \frac{\int T_e N_i n_e \mathrm{d}V}{\int N_i n_e \mathrm{d}V}$$
(3.36)

defined for each ion N_i , using the *r.m.s.* temperature fluctuation

$$t^{2}(N_{i}) = \frac{\int (T_{e} - T_{o}(N_{i}))^{2} N_{i} n_{e} \mathrm{d}V}{T_{o}(N_{i})^{2} \int N_{i} n_{e} \mathrm{d}V}.$$
(3.37)

From comparison of temperatures measured by different methods, this temperature fluctuation scheme led to conclude that temperature fluctuations are common in nebulae, with typical values of $t^2 = 0.03 - 0.05$ (see references in Peimbert 1996, Stasińska 1998, Mathis et al. 1998, Esteban 2002). The case is not always easy to make: the determination of the continuum in the vicinity of the Balmer jump is difficult, the combination of data from different instruments for the comparison of far infrared data with optical ones involves many potential sources of errors, lines of O⁺⁺ and of H are not emitted in coextensive zones etc ... Nevertheless, the observational results seem overwhelming. And, as noted by Peimbert (2002), the value of t^2 found in such a way is never negative!

Note that in the PNe NGC 6153, NGC 7009, M1-42 and M2-36, (Liu et al. 1995, 2000, 2001, Luo et al. 2001) much larger values of t^2 , of the order of 0.1, would be derived from the comparison of optical recombination lines (ORL) to collisionally excited lines (CEL). But this may be another problem (see Sect. 3.6).

A value of $t^2 \sim 0.04$, in the scheme of Peimbert (1967), typically leads to an underestimation of O/H by about 0.3 dex \dagger . It is thus extremely important to determine whether temperature fluctuations exist or whether they are an artefact of the techniques employed. And, if they really exist, to understand their nature and possibly derive some systematics to account for them in abundance derivations. Note that, so far, the evidences are always *indirect*, based on the comparison of different methods to estimate T_e . Only mapping the nebulae with appropriate sensitivity and spatial resolution in the temperature diagnostic lines could give *direct* evidence of small scale fluctuations. In the planetary nebula NGC 6543, HST mapping of [O III] $\lambda 4363/5007$ shows much smaller spatial temperature variations than expected for this object from indirect measurements (Lame et al. 1998). In NGC 4361, long slit spectroscopy gives a *surface* temperature fluctuation $t_s^2 \sim 0.002$ (Liu 1998). In Orion, long slit mapping of the Balmer decre-

 $[\]dagger$ N/O and Ne/O ratios are less affected by temperature fluctuations than N/H, since N/O and Ne/O abundance determinations rely on lines with similar temperature dependences and emitted in roughly the same zones.

ment gives $t_s^2 \sim 0.001$ (Liu et al. 1995a). All these observed t_s^2 translate into volume temperature fluctuations $t^2 \leq 0.01$.

Actually, the value of t^2 defined by Eq. (3.37) is not strictly speaking equal to the value of t^2 derived observationally, for example from the comparison of temperatures derived from [O III] $\lambda 4363/5007$ and from the Balmer jump. Kingdon & Ferland (1995) introduced the notation t_{str}^2 for the former (str meaning "structural") and t_{obs}^2 for the latter. Photoionization models of planetary nebulae and H II regions generally fail to produce such large values of t_{obs}^2 as observed in real nebulae (e.g. Kingdon & Ferland 1995, Pérez 1997), except in the case of high metallicities, i.e. equal to the canonical "solar" value or larger. Note that in this case, what produces t_{obs}^2 in the model is actually the temperature gradient discussed above. Density fluctuations could be a source of temperature fluctuations, due to increased collisional deexcitation in zones of higher density, but photoionization models including such density fluctuations also fail to return large enough values of t^2 (Kingdon & Ferland 1995). Note that introducing a density condensation shifts the dominant oxygen ion to a less charged one, and consequently the increase in $t^2(O^{++})$ is not as important as might have been thought a priori. Viegas & Clegg (1994) argued that very high density clumps $(n > 10^5 \text{ cm}^{-3})$ could mimic the effects of temperature fluctuations by collisionally deexciting the [O III] λ 5007 line. The existence of such clumps is however not confirmed by the densities derived from [Ar IV] $\lambda 4740/4711$, from the ratio of fine structure [O III] lines and from high order Balmer decrement lines (Liu et al. 2000, 2001). Note that, if they existed, such clumps should be located very close to the star in order to emit significantly in [O III] $\lambda 5007$ with respect to the rest of the nebula.

As will be discussed in Sect. 3.6, abundance inhomogeneities have been proposed to solve the ORL / CEL problem (Torres-Peimbert et al. 1990, Péquignot et al. 2002). Carbon and/or oxygen rich pockets would produce zones of lower temperature (due to increased cooling). In PNe the existence of carbon rich pockets is attested from direct observations in at least a few objects (e.g. Abell 30 and Abell 78, Jacoby & Ford 1983) and these carbon rich inclusions are thought to be material coming from the third dredge up in the progenitor star (Iben et al. 1983). But the existence of oxygen rich pockets in PNe is more difficult to understand from the present day evolution models for intermediate mass stars (see Sect. 5). On the other hand, in H II regions, especially in giant H II regions, oxygen rich pockets could be made of material ejected by Type II supernovae and not yet mixed with the gas (Elmegreen 1998).

Other origins of temperature fluctuations have also been proposed, involving additional heating processes. The fact that several detailed photoionization studies of planetary nebulae (Peña et al. 1998) or giant H II regions (García-Vargas et al. 1997, Stasińska & Schaerer 1999, Luridiana, et al. 1999, Luridiana & Peimbert 2001, Relaño et al. 2002) predict significantly lower [O III] $\lambda 4363/5007$ ratios than observed indeed argues for additional heating. Shock heating or conductive heating are among the possibilities to investigate. Heat conduction from hot bubbles has been examined by Maciejewski et al. (1996) and shown to be insufficient to explain the t^2 derived from observations. The energy requirements to produce the observed values of t^2 have been evaluated by Binette et al. (2001) in the hypothesis of hot spots caused by an unknown heating process. In H II regions, the mechanical energy associated with the ionizing sources (stellar winds, supernova explosions) does not seem sufficient to produce the required value of t^2 (Binette et al. 2001, Luridiana et al. 2001). In planetary nebulae, a considerable amount of kinetic energy is available from the central star winds. The radiative hydrodynamical models of Perinotto et al. (1998) present a temperature spike at the external shock front. This temperature increase, located in a relatively narrow external zone, is not

expected to produce a higher [O III] $\lambda 4363/5007$ temperature than derived from the Balmer jump. In the radiative hydrodynamical models computed by Mellema & Frank (1995) for aspherical nebulae, there are areas of lower density in which cooling is inefficient and the temperature is higher due to shock heating. Mellema & Frank suggest that this may explain the differences in temperatures derived from different methods. However, a quantitative analysis remains to be done in order to check whether the predicted effect indeed reproduces what is observed. Simulations taking into account the evolution of the velocity and mass-loss rate of the fast central star wind (Dwarkadas & Balick 1998) lead to considerably more structure on smaller scales, which could be even more favorable to solve the temperature fluctuation problem. In a slightly different context, Hyung et al. (2001) have tried to explain the high temperature observed in the inner halo of NGC 6543, (15 000 K as opposed to 8 500 K for the bright core) by means of a simulation using a hydrodynamic code coupled to a photoionization calculation. These authors showed that mass loss and velocity variations in the AGB wind can simultaneously explain the existence of shells in the halo and the higher O⁺⁺ temperature.

Recently, Stasińska & Szczerba (2001) proposed a completely different origin for temperature fluctuations, related to photoelectric heating by dust grains. This hypothesis is also very promising and can be checked observationally (see Sect 3.7.5).

Although the t^2 scheme has proved very useful to uncover the possibile existence of temperature inhomogeneities, it may not be appropriate to describe the real situation. In the case where abundance inhomogeneities are the source of the temperature variations the Peimbert (1967) description is obviously inadequate. But it can also be inappropriate for nebulae of homogeneous chemical composition, as shown on a simple two-component toy model. Consider two homogeneous zones of volumes V_1 and V_2 with temperatures T_1 and T_2 , electron densities n_1 and n_2 , and densities of the emitting ions (e.g. O^{++}) N_1 and N_2 . Calling f the ratio $(N_2n_2V_2)/(N_1n_1V_1)$ of the weigths of the emitting regions, the mean electron temperature defined by Peimbert (1967) can be expressed as:

$$T_0 = \frac{T_1 + fT_2}{1+f} \tag{3.38}$$

and t^2 as:

$$t^{2} = \frac{(T_{1} - T_{0})^{2} + f(T_{2} - T_{0})^{2}}{(1 + f)T_{0}^{2}}.$$
(3.39)

For $T_0=10\,000$ K, the case f=1 (i.e. regions of equal weight) corresponds to $T_1=12\,000$ K and $T_2 = 8000$ K. It must be realized that this 4000 K difference in temperatures requires a difference of a factor 3 in the heating or cooling rates between the two zones. When $f \gg 1$, there is a high weight zone at $T_2 \leq T_0$ and a low weight zone at $T_1 \gg T_0$. Such a situation could correspond to a photoionized nebula with small volumes being heated by shocks or conduction. When $f \ll 1$, there is a high weight zone at $T_1 \ge T_0$ and a low weight zone at $T_2 \ll T_0$ which could correspond to high metallicity clumps. With such a toy model, one can explore the biases in abundance obtained for O^{++} using the [O III] $\lambda 4363/5007$ temperature and different lines emitted by this ion. Examples are shown in Figs. 8 and 9 of Stasińska (2002). Following expectations, O^{++} derived from [O III] λ 5007 is generally underestimated, but it is interesting to note that the magnitude of the effect depends both on f and on T_0 . The bias is very small when $T_0 \gtrsim 15\,000$ K. It is small in any case if f > 3 - 4, because [O III] $\lambda 4363$ saturates above ~ 50000K. At T_0 ~ 8000 K, O⁺⁺ is underestimated by up to a factor of 2–3 in the regime where [O III] λ 4363 is significantly emitted in both zones. As expected, O⁺⁺ derived from infrared fine structure lines and from the optical recombination line O II $\lambda 4651$ is correct. Such a toy model demonstrates that the classical temperature fluctuation scheme can be misleading.

Even in a simple two zone model, the situation needs at least three parameters to be described, not two. In our representation, these parameters would be T_1 , T_2 and f, but other definitions can be used.

3.6. The optical recombination lines mystery

It has been known for several decades that optical recombination lines in PNe and H II regions indicate higher abundances than collisionally excited lines (see Liu 2002 for a review). Most of the former studies concerned the carbon abundance as derived from C II λ 4267 and from C III] λ 1909, but more recent studies show that the same problem occurs with lines from O⁺⁺, N⁺⁺ and Ne⁺⁺ (Liu et al. 1995b, 2000, 2001, Luo et al. 2001). The ORL abundances are higher than CEL abundances by factors of about 2 for most PNe, discrepancies over a factor 5 are found in about 5 % of the PNe and can reach factors as large as 20 (Liu 2002). For a given nebula, the discrepancies for the individual elements C, N, O, Ne are found to be approximately of the same magnitude.

The explanations most often invoked are: i) temperature fluctuations, ii) incorrect atomic data, iii) fluorescent excitation, iv) upward bias in the measurement of weak line intensities, v) blending with other lines, vi) abundance inhomogeneities. None of them is completely satisfactory, some are now definitely abandoned.

The completion of the OPACITY project has allowed accurate computation of effective recombination coefficients needed to analyze ORL data. The advent of high quantum efficiency, large dynamic range and large format CCDs now allows to obtain high quality measurements of many faint recombination lines for bright PNe, thus hypothesis iv) cannot be invoked anymore. In addition, Mathis & Liu (1999) have measured the weak $[O \text{ III}] \lambda 4931$, whose intensity ratio with $[O \text{ III}] \lambda 5007$ depends only on the ratio of transition probabilities from the upper levels. They found $(4.15 \pm 0.11) \ 10^{-4}$ compared to the theoretical values 4.09 10^{-4} (Nussbaumer & Storey 1981), 4.15 10^{-4} (Froese Fisher & Saha 1985), $2.5 \ 10^{-4}$ (Galavís et al. 1997). If, as expected, the latter computations give the more accurate results, the bias in the measurement of extremely weak lines could amount to 60%. This is far below what is needed to explain the ORL/CEL discrepancy. A large number of faint recombination lines have now been measured, and the observed relative intensities of permitted transitions from C^{++} , N^{++} , O^{++} and Ne^{++} are in agreement with the predictions of recombination theory, which goes against ii), iii), iv) and v). As mentioned in the previous subsection, the values of t^2 derived from the comparison of temperatures from [O III] $\lambda 4363/5007$ and from the Balmer jump are too small to account for the large abundances derived from the ORL, therefore i) does not seem to be the good explanation. This is true even adopting a two-zone toy model instead of Peimbert's fluctuation scheme.

On the basis of detailed studies of several PNe, Liu (2002) notes that for a given nebula, the discrepancies for the individual elements C, N, O, Ne are found to be approximately of the same magnitude. The ORL/CEL abundance ratios correlate with the difference between the temperatures from [O III] $\lambda 4363/5007$ and from the Balmer jump. Liu et al. (2000) favour the hypothesis of an inhomogeneous composition, with clumps having He/H = 0.4 and C, N, O, Ne abundances around 400 times that in the diffuse gas in the case of NGC 6153. It is indeed possible to construct a photoionization model with components of different chemical composition that reproduces the observed integrated line ratios satisfactorily (Péquignot et al. 2002). However, such a model is difficult to reconcile with the present theories of element production in intermediate mass stars (e.g. Forestini & Charbonnel 1997). Also, such super metal rich knots are not in pressure equilibrium with the surroundings and should be short lived, unless they are very dense.

Spatial analyses of NGC 6153 (Liu et al. 2000) and of NGC 6720 (Garnett & Dinerstein

2001) show that the ORL/CEL discrepancy decreases with distance to the central star. A possible explanation for the large intensities of the recombination lines of C, N, O, Ne, mentioned by Liu et al. (2000), is high temperature dielectronic recombination for states with high quantum numbers, a process so far not included in the computations of the effective recombination coefficients. Then, the ORL would be preferentially emitted in regions of temperatures of $(2-5) 10^4$ K. There remains to find a way to obtain such high temperature material in planetary nebulae. Apart from conduction and shock fronts, there is also the possibility of heating by dust grains (see Sect. 3.7.7).

3.7. The role of internal dust

Until now we have omitted the solid component of nebulae, which, although not important by mass (usually of the order of 10^{-3} , see Hoare et al. 1991, Natta & Panagia 1981, Stasińska & Szczerba 1999) importantly affects the properties of PNe and H II regions. The discussion below deals only with aspects that are explicitly linked with the derivation of the chemical composition of nebulae.

3.7.1. Evidence for the presence of dust in the ionized regions

Numerous mid- and far- IR spectral observations of PNe and H II regions have shown the presence of a strong continuous emission at a temperature around 100 - 200 K, attributed to dust grains heated by the ionizing stars (see the discussion in Pottasch 1984). Near- and mid-IR array observations have shown that the distribution of this emission is comparable to the distribution of [Ne II] $\lambda 12.8 \,\mu m$ and [S IV] $\lambda 10.5 \,\mu m$ radiation, implying that dust is not only found in the neutral outskirts, but also inside the ionized regions (see review by Barlow 1993). This does not necessarily imply, however, that grains are intimately mixed with ionized gas. A priori, they could be located exclusively in tiny, dusty neutral clumps, such as observed in the Helix nebula NGC 7293 (e. g. O'Dell & Handron 1996) or in the Ring Nebula NGC 6720 (Garnett & Dinerstein 2001). A crucial piece of evidence is provided by the following argument. It has been demonstrated by Kingdon et al. (1995) and Kingdon & Ferland (1997) that, in nebulae of normal chemical composition, numerous lines of elements such as Mg, Al, Ca, Cr, Fe, should be detectable in ultraviolet or optical spectra. What observations show is that these elements are depleted in PNe by factors around 10 – 100 (Shields 1978, Shields et al. 1981, Shields 1983, Harrington & Marionni 1981, Volk et al. 1997, Perinotto et al. 1999, Casassus et al. 2000). The same holds for H II regions (Osterbrock et al. 1992, Esteban et al. 1998).

3.7.2. Heavy element depletion

One important consequence of the above mentioned observational fact is that analyses of ionized nebulae do not provide the real abundance of such elements as Mg, Al, Ca, Cr, Fe, which can be incorporated in grains. Carbon can also be significantly depleted in carbon-rich grains – graphite or PAHs. The measurement of carbon abundances from nebular lines therefore gives only a lower limit to the total carbon content. This is also true for oxygen, although to a much smaller extent. In H II regions it is possible to estimate the amount of oxygen trapped in dust grains from the observation of the Mg, Si and Fe depletions (see Esteban et al. 1998). Also, the consideration of the Ne/O ratio can be useful, since Ne, being a noble gas, cannot enter in the composition of grains.

3.7.3. The effect of dust on the ionization structure

Dust internal to H II regions and PNe competes with the gas in absorbing Lyman continuum photons, therefore lowering the H β luminosity. The nebular ionization structure is affected by two competing processes. The ionization parameter drops due to the

fact that part of the Lyman continuum photons are absorbed by dust and not by gas. This alone would tend to lower the general ionization level. The ionizing radiation field seen by the atomic species depends on the wavelength dependence of the dust absorption cross section. For conventional dust properties, the absorption cross section per H nucleon smootly decreases for energies above 13.6 eV (see e.g. Fig. 1 from Aanestad 1989), favouring the ionization of He with respect to H. In the model of the Orion nebula presented by Baldwin et al. (1991), the net effect of absorption by dust is to bring the H⁺ and He⁺ zones into closer agreement.

3.7.4. The effect of dust obscuration on the emission line spectrum

The presence of dust inside the ionized regions affects the emission line spectrum by selectively absorbing (and scattering) the emitted photons. Since the emission lines from various ions are formed in different zones, their relative fluxes as measured by the observer do not only depend on a general extinction law, but also on the differences in the geometrical paths of the photons in the different lines. This, in principle, can be modelled using a photoionization code including dust but the problem is complex and the solution extremely geometry-dependent. For practical purposes, as explained in Sect. 3.3, it is more convenient to deredden an observed spectrum by adjusting the observed Balmer decrement to a theoretical one. If comparisons need to be made with a photoionization model, then they should be made with the theoretical emitted spectrum without dust attenuation. Of course, such a procedure is only approximate.

Resonance lines have an increased path length with respect to other lines, and are therefore subject to stronger absorption by dust. This is the case of H Ly α , which may be entirely trapped by grains in the case of very dusty nebulae (Ly α absorption is actually one of the main heating agents of dust particles in planetary nebulae, see e.g. Pottasch 1984). Other resonance lines, such as C IV λ 1550, N V λ 1240 or Si IV λ 1400, are also affected by this selective absorption process. Usually, an escape probability formalism is used to account for it (Cohen et al. 1984). The observed intensity of the resonance lines depends on the amount of dust, on the ionization structure and on the velocity fields both in the nebula and in the surrounding halo and intervening interstellar medium (see e.g. Middlemass 1988). The inclusion of dust attenuation in a tailored photoionization model of the PN NGC 7662 results in a derived gas phase C abundance twice as large as would be deduced using classical methods (Harrington et al. 1982).

Another consequence of selective dust absorption is that it prevents the 100 % conversion of high-n Lyman lines into Ly α and Balmer lines (the case B). For dusty environments such as the Orion Nebula, the H β emissivity can be reduced by 15 % (Cota & Ferland 1988).

3.7.5. The effects of grains on heating and cooling of the gas

An obvious effect of the presence of grains on the thermal balance of ionized nebulae, is due to the depletion of strong coolants such as Si, Mg, Fe, which enhances the electron temperature with respect to a dust-free situation. This aspect is important not only for detailed model fitting of nebulae, but also when using grids of photoionization models to calibrate strong line methods for abundance determinations (Henry 1993, Shields & Kennicutt 1995).

Grains have also a *direct* influence on the energy balance. The photoelectric effect on dust grains has been shown by Spitzer (1948) to be a potential heating source in the interstellar matter. Baldwin et al. (1991) have introduced the physical effects of dust in the photoionization code CLOUDY. They constructed a detailed model of the Orion nebula and found that in this object, heating by photoelectric effect can amount to a

significant proportion of the total heating while collisions of the gas particles with the grains contribute somewhat to the cooling.

The effect of dust heating is dramatic in the H-poor and extremely dusty planetary nebula IRAS 18333-2357 in which $m_{\rm d}/m_{\rm H}$ is estimated around 0.4 (Borkowski & Harrington 1991). In this object, heating is almost entirely due to photoelectric effect.

In nebulae in which dust-to-gas mass ratio, dust properties and grain size distributions have the canonical values, the relative importance of dust heating is generally not very large. If, however, there is a large proportion of *small* dust grains, then the contribution of dust heating to the total energy gains may become important, as demonstrated by Dopita & Sutherland (2000) on a grid of dusty photoionization models of planetary nebulae. The effect is more pronounced in the central parts of the nebulae, being proportional to the mean intensity of the ultraviolet radiation field, and gives rise to a strong temperature gradient.

If such small grains do exist (and there is now growing evidence for that (Weingartner & Draine, 2001), their presence in planetary nebulae would solve a number of problems that have found no satisfactory solution so far (see Stasińska & Szczerba 2001): i) the thermal energy deficit inferred in some objects from tailored photoionization modelling; ii) the large negative temperature gradients inferred directly from spatially resolved observations and indirectly from integrated spectra in some PNe; iii) the Balmer jump temperatures being systematically smaller than temperatures derived from forbidden lines; iv) the intensities of $[O I] \lambda 6300$ often observed to be larger than predicted by photoionization models: indeed, near the ionization front, Lyman continuum photons are exhausted and the only photons still present are photons below the Lyman limit. Those are not absorbed by hydrogen but can heat the gas via photoelectric effect on dust grains. One should however remember that dust is not the only way to enhance [O I] emission, other mechanisms have been mentioned in Sect. 1.1.

The energy gains per unit volume of gas due to photoelectric effect, G_d , are proportional to the number density of dust grains and to the intensity of the stellar radiation field. Combining with Eq. (1.16) which expresses the gains due to photoionization of hydrogen, G_H , it is easy to show that G_d/G_H is proportional to $(m_d/m_H)U$, where Uis the ionization parameter. This has important consequences in the case of filamentary structures. If small grains are present, the photoelectric effect will boost the electron temperature in the low density components. This will result in important small-scale temperature variations in the nebula. The models of Stasińska & Szczerba (2001) show that *moderate* density inhomogeneities (such as inferred from high resolution images of PNe) give rise to values of t^2 similar to the ones obtained from observations. Note that, contrary to the dust-free case, the tenuous component has a higher T_e than filaments or clumps, therefore the clumps are better confined.

Stasińska & Szczerba (2001) also point out that if, as expected, dielectronic recombinations for high level states strongly enhance the emissivities of recombination lines, the presence of small grains in filamentary planetary nebulae would boost the emission of recombination lines from the diffuse component, principally in the inner zone. Therefore, small grains could solve in a natural way both the temperature fluctuation problem and the ORL/CEL discrepancy.

The presence of small grains in planetary nebulae can be tested observationally by measuring the temperature *in* and *between* filaments.

3.8. The specific case of the helium abundance determination

The determination of the helium abundance follows the same principles as that of other elements. But one is much more demanding about the accuracy. To follow the production

of helium in stars, and the evolution of the helium content in galaxies, 10% accuracy is a goal that one would like to achieve. Helium abundances compiled from the literature over the years must be considered with caution, because of the different treatments adopted by various authors. On the other hand, the required accuracy should be reachable with consistent observations and modern data treatments. To determine the primordial helium abundance, Y_p , one needs a much better accuracy, since quite different cosmologies are predicted for values Y_p differing by a only few percent. From low metallicity giant extragalactic H II regions, Olive et al. (1997) find $Y_p = 0.234 \pm 0.002$ while Izotov & Thuan (1998) find $Y_p = 0.244 \pm 0.002$. These two estimates are mutually exclusive. Is it possible to say which of the two - if any - is correct?

The first step is to obtain the intrinsic values of the intensities of the helium and hydrogen lines in an observed spectrum. If the spectrum contains stellar light, as in the case of giant H II regions, one must correct the observed intensities for underlying stellar absorption. The recent evolutionary synthesis models of Gonzalez Delgado et al. (1999) provide a theoretical framework for that. One also has to correct the intensity ratios for reddening, assuming a given reddening "law" and a given intrinsic value of the ratios of the hydrogen line intensities. The latter mainly depends on the electron temperature, which can be estimated from the [O III] $\lambda 4363/5007$ ratio, with a correction due the fact that the O^{++} region is only a part of the H^+ region. Using an appropriate number of lines, one can estimate iteratively the reddening and the correction for underlying absorption (e.g. Izotov & Thuan 1998). However, as commented by Davidson & Kinman (1985) and Sasselov & Goldwirth (1995), and as mentioned in Sect. 3.3, collisional excitation of H Balmer lines may become important, especially in H II regions of high T_e . So far, this effect has always been omitted in the determination of the abundance of primordial He. It may induce an overestimation of the reddening, and therefore an underestimation of the He⁺ abundance derived from He I λ 5876 by up to 5 % (Stasińska & Izotov 2001). The importance of this effect depends on the abundance of residual H⁰.

Then, from the corrected ratios of emission lines one has to determine the value of He^+/H^+ , or, to be more exact, of $\int n(\text{He}^+) dV / \int n(\text{H}^+) dV$. This assumes that the line emissivities do not vary strongly over the nebular volume. The emissivities depend on T_e , and also on n_e in the case of some helium lines, due to enhancement by collisional excitation from the metastable 2^{3} S level. If one knows n_{e} from plasma diagnostics, the contribution of collisional excitation can be obtained. The recent tables of Benjamin et al. (1999), based on a resolution of the statistical equilibrium of the He atom using the best available atomic data, can be used for this purpose. Note that these authors also provide analytical fits, with the warning that some of them lead to values that may differ by 1%or more from the actually computed values of the emissivities. Some He line emissivities are also affected by self absorption of the pseudo resonance lines from the 2^{3} S level. Using a sufficient number of helium lines, one can in principle determine iteratively and selfconsistently the characteristic temperature and density of the helium line emission, and the relative abundance of He⁺. The treatment of radiation transfer in the lines remains to be improved and is announced as a next step by Benjamin et al. (1999). However, this is a complex problem: it depends on the velocity field and on the amount of internal dust which selectively absorbs resonant photons. Therefore, one does not expect models to be easily applicable to real objects. However, since this is a second order effect, this is perhaps not too problematic, if one discards the lines likely to be most affected by this process. One must not forget that the emissivities of the H Balmer lines too may be in question, both because of the contribution of collisional excitation mentioned above and because the presence of dust deviates the hydrogen spectrum from case B (see Hummer & Storey 1992). Another problem is to take into account the non uniformity of T_e . Sauer &

Jedamczik (2002) have computed a grid of photoionization models for this purpose, and introduce the concept of a "temperature correction factor" which they compute in their models. Note, however, that the real temperature structure of nebulae is not obtained from "first principles", as the preceding sections made clear. Therefore, the distribution of T_e in real objects has most probably a larger impact than predicted by the models of Sauer & Jedamczik (2002). Peimbert et al. (2002) have adopted a semi-empirical approach, based on the Peimbert's (1967) temperature fluctuation scheme. But the temperature fluctuation scheme may give spurious results in the hypothesis of zones of highly different temperatures, as argued in Sect. 3.5.2.

If He II lines are present in the spectra, they have to be accounted for, to determine $\int n(\text{He}^{++}) dV / \int n(\text{H}^+) dV$. The major uncertainty in that case comes probably from the lack of knowledge of the temperature characterising the emission of He II lines. An additional difficulty is due to the fact that part of the He II emission may be of stellar origin.

The He/H abundance is obtained after considering ionization structure effects. For low values of the mean effective temperature of the radiation field, a zone of neutral helium is present. Unfortunately, no ionization correction formula can be safely applied, since the ionization structure of helium with respect to hydrogen mainly depends on the hardness of the radiation field, while the ionization structure of the heavy elements also strongly depends on the gas distribution (e.g. Stasińska 1980b). In the case of an H II region ionized by very hot stars, photoionization models show that the He⁺ region may on the contrary extend further than the H⁺ region (see for example Stasińska 1980b or Sauer & Jedamczik 2002). Whether this is the case for an object under study should be tested by models.

Olive & Skillman (2001) stress the importance of having a sufficient number of observational constraints and of using them in a self consistent manner with a Monte-Carlo treatment of all sources of errors. Unfortunately, the errors on the temperature structure and on the ionization structure of real nebulae are very difficult to evaluate, and this, combined with uncertainties in atomic parameters and deviations from case B theory implies that the uncertainty in derived helium abundances is certainly larger than claimed.

4. Observational results on abundances in H II regions of the Milky Way

4.1. The Orion nebula: a benchmark

The Orion nebula is the brightest and most observed H II region in the galaxy. Therefore it is a benchmark in many respects. O'Dell (2001) and Ferland (2001) have summarized our present knowledge on this object. In the following, we only discuss aspects related to the chemical composition in the ionized gas.

It is of interest, beforehand, to mention that it is with the Orion nebula that the concept of filling factor started. Using a spherical representation, Osterbrock & Flather (1959) showed that the optical surface brightness data could be reconciled with the observed [O II] $\lambda 3726/3729$ intensity ratios only when assuming extreme density fluctuations. They proposed a schematic model in which these fluctuations are represented as condensations immersed in a vacuum, with the relative volume of the condensations being only 1/30 of the total volume of the nebula. But a more realistic model of the Orion nebula (Zuckerman 1973, Balick et al. 1974, see also discussion in O'Dell 2001) is to represent the Orion nebula as an ionized blister on a background molecular cloud. From a detailed

	Не	С	Ν	Ο	Ne	Mg	Si	S	Ar	Fe	Ni
a b c d e f g	$ \begin{array}{r} 100000 \\ 90000 \\ 101000 \\ 97700 \\ 100000 \end{array} $	280 210 250 250	68 87: 52: 60 42		-	3.2:	4.5	$8.5 \\13.3 \\9.4 \\14.8 \\9.3 \\8.6$	2.1 2.6 6.3 3.3	2.7: 1.3	0.14:

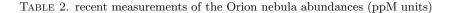
a Rubin et al. (1991, 1993), optical + IR spectroscopy, model

b Baldwin et al. (1991), long slit optical + IR + UV spectroscopy, model

c Osterbrock et al. (1992), optical spectroscopy, empirical d Esteban et al. (1998) ($t^2 = 0.024$), optical spectroscopy, empirical e Esteban et al. (1998) ($t^2 = 0.0$), optical spectroscopy, empirical

f Simpson et al. (1998), IR spectroscopy, empirical

g Deharveng et al. (2000), optical integrated spectroscopy, empirical



comparison of the H β surface brightness map and of the [S II] $\lambda 6731/6717$ map. Wen & O'Dell (1995) derived a 3D representation of the nebula. The ionized skin is very thin with respect to the overall size of the nebula, which justifies the plane parallel approximation for photoionization modelling.

The extinction in the Orion nebula is well known to differ from the standard reddening law, and has been studied in detail (see Baldwin et al. 1991, Bautista et al. 1995, Henney 1998 for recent references)

Abundances have been derived both from T_e -based empirical methods and from photoionization models, using optical data with increased signal to noise and spectral resolution, with the addition of ultraviolet data obtained with IUE (and more recently with HST) and infrared data from ground-based telescopes and from KAO, ISO, and MSX. Table 2 summarizes the abundances derived during the last decade. All the abundances are given in ppM units $(10^6 \times \text{the number of particles of a given species with respect to})$ hvdrogen)

There is rather good agreement for the oxygen abundances, the value of Esteban et al. (1998) with $t^2 = 0$ being the lowest and the one with $t^2 = 0.024$ being the highest. Note that the preferred abundances of Esteban et al. (1998) are those obtained with $t^2=0.024$, which is the value indicated by the ORL/CEL comparison. However, the comparison of the [O III] $\lambda 4363/5007$ and Balmer jump temperatures is consistent with $t^2 = 0$. One must be aware that abundances from models are not always the most reliable, since the models do not reproduce the ionization structure perfectly. The values of Simpson et al. (1998) for Ne, S, and Ar are obtained from simultaneous observations of the most abundant ionic stages.

The Mg, Si, Fe and Ni abundances are heavily depleted with respect to the Sun (indicating the presence of grains intimately mixed with the gas phase in the ionized region). There is actually a controversy with respect to the interpretation of Fe lines (Bautista et al. 1994, Baldwin et al. 1996, Bautista & Pradhan 1998). Esteban et al. (1999) recommend to derive Fe abundances from Fe⁺⁺ lines as done in the works quoted in Table 2.

G. Stasińska: Abundances in H II regions and planetary nebulae

	He	\mathbf{C}	Ν	Ο	Ne	Mg	Si	\mathbf{S}	Ar	\mathbf{Fe}	Ni
Su	ın										
a	98000:	363	112	851	123:	38	35	16	3.6:	47	1.8
b	85000:	331	83	676	120:	38	35	21	2.5:	32	1.8
с		391	85	544		34	34			28	
d				490							
Ga	as phase	local i	nterste	llar me	edium						
e		141	75	319		22	19.5	16.6		7.4	0.26
Be	e stars										
f		224	44.5	407							
g		190	64.7	350		23.0	18.8			28	
	Anders &		· · · ·	/							
	Grevesse		val (199)	8)							
	Holweger	· /	1 (0)	201)							
	Allende P		<pre></pre>	/		(1007)	(\mathbf{N}) \mathbf{C}	6	1 (100	7) (C)	Condoll:
	Meyer et al. (1996	· · · ·		, ,		· · ·	()/		<pre></pre>	/ \ //	
	unha & 1			Savage	(1990)	(51, 5,	re, m)	Sona a	c (mey	2001) (Mg)
	Compilati			& Mey	er (200	1)					
5	Computati		ii Sona	w mey	~ (200	±,					

TABLE 3. Solar vicinity abundances (ppM units)

4.2. Abundance patterns in the solar vicinity and the solar abundance discrepancy

Stars and nebulae provide a different perspective of the solar vicinity chemical composition. The methods for abundance determinations differ (and might be in error in different ways) and the astrophysical significance of the abundances is not necessarily the same. One expects a priori the surface composition of the Sun to be identical with that of other objects in the solar vicinity. It turns out that the abundances from nearby H II regions (Orion being the best example) are significantly smaller than the solar abundances from the works of Anders & Grevesse (1989) or Grevesse & Sauval (1998). It is to be noted that, despite of this fact, the reference abundance is often chosen to be that of the Sun from Anders & Grevesse (1989). Table 3 summarizes the abundances in the Sun, in the local interstellar medium (ISM) and in local B stars from recent references.

Peimbert et al. (2001) notes that a decade ago, the oxygen abundance in the Sun was 0.44 dex higher than in Orion but when using the value from Esteban et al. (1998) with $t^2 = 0.024$ and the solar value of Grevesse & Sauval (1998), the difference is only 0.19 dex. When accounting for the fraction of oxygen that is contained in dust grains (which can be done assuming a standard chemical composition of the dust grains, and the constraints provided by the Mg, Si and Fe abundances), the oxygen abundance is multiplied by a factor 1.2 and the difference between the Solar value and Orion is only 0.11 dex.

The oxygen abundance in Orion obtained with $t^2 = 0$ is actually similar to the one in the local interstellar medium (obtained from high resolution and high signal to noise absorption measurements, Meyer et al. 1998) and in local B stars (e.g. Cunha & Lambert 1994). Several possible explanations have been invoked. The ones listed by Meyer et al. 1998 are: i) an early enrichment of the Solar system by a local supernova (not really tenable if the abundances of *all* the elements in the local ISM are 2/3 solar); ii) a recent

28

infall of metal poor gas in the local Milky Way; iii) an outward diffusion of the Sun from a smaller Galactocentric distance. A more recent discussion Sofia & Meyer (2001) definitely rejects the hypothesis of the local ISM standard being 2/3 of the Sun. Indeed, new determinations give much smaller values for O/H: 544 ppM (Holweger 2001), 490 ppM (Allende Prieto et al. 2001). The support for the 2/3 solar value is also invalidated from carbon (see their discussion). Note that Sofia & Meyer (2001) also argue that B stars have metal abundances that are *too low* to be considered valid representations of the ISM. According to Meyer et al. (1998), the local standard oxygen abundance should be 540 ppM (gas + dust).

In conclusion, the "solar abundance discrepancy" has gradually disappeared, mostly because modern derivations of the solar oxygen abundance give much lower values than earlier ones. This reinforces confidence in H II regions as probes of the ISM abundances and in the methods used to analyze them. This is good news, since H II regions are practically the only way to derive oxygen abundance in external galaxies, if one excepts the abundance analysis in giant stars of local galaxies which require very large telescopes. Giant H II regions can be used as abundance indicators up to large redshifts (see Pettini in the same volume).

4.3. Abundance gradients in the Galaxy from H II regions

Abundance gradients in disk galaxies constitute one of the more important observational constraints for models of galaxy chemical evolution. As a matter of fact, abundance gradients were first recognized to exist in external galaxies, where radial trends of emission line ratios were noted as far back as in the fourties (Aller 1942) and were attributed to abundance gradients in the early seventies (Searle 1971, Shields 1974).

In our own galaxy, gradients are more difficult to determine, due to distance uncertainties and because many H II regions are highly obscured by dust lying close to the galactic plane. The first determination of an abundance gradient in our galaxy from H II regions was made by Peimbert, Torres-Peimbert & Rayo (1978). It is worth the effort to derive abundance gradients in the Milky Way because it is a benchline for chemical evolution of galaxies. Only in the Milky Way can one have direct access to abundance measurements from so many sources as H II regions, planetary nebulae, individual B, F, G stars etc..., which all probe different epochs in the Milky Way history. Esteban & Peimbert (1995) and Hou et al. (2000) provide excellent reviews on this topic. Table 4 presents a compilation of Galactic abundance gradients from H II regions in units of d $\log(X/H)$ / dR in kpc⁻¹. Column 9 indicates the spanned range of galactocentric distances in kpc. Column 10 lists the total number of objects used to derive the gradients. Note that the errors quoted for the gradients include only the scatter in the nominal values of the derived abundances about the best fit line. They do not take into account the uncertainties in the abundances and the possible errors on the galactocentric distances. Most abundances were obtained using empirical methods.

It must be noted that, even in the case of similar methods, some details in the procedures employed may lead to significantly different results. For example, the much larger oxygen gradient found by Peimbert et al. (1978) probably results from their using the temperature fluctuation scheme (with $t^2 = .035$).

A possible flattening of abundance gradients in the outer disk has been mentioned by Fich & Silkey (1991) and Vilchez & Esteban (1996) but Rudolph et al. (1997) and Deharveng et al. (2000) find no clear evidence for that.

The situation with the N/O ratio is not clear. N/O ratios determined from N^{++}/O^{++} using far infrared (FIR) lines (Simpson et al. 1995, Afflerbach et al. 1997, see also Lester et al. 1987 and Rubin et al. 1988) are up to twice the values derived from N^+/O^+ using

30	G	. Stasińska	: Abundan	ces in H II	regions ar	id planetar	ry nebulae		
	He	С	Ν	0	Ne	S	Ar	range	nb
a	$\begin{array}{c} 0.02 \\ \pm \ 0.01 \end{array}$		-0.23 ± 0.06	-0.13 ± 0.04				8-14	5
b	-0.001 ± 0.008		-0.090 ± 0.015	-0.070 ± 0.015		-0.010 ± 0.020	-0.060 ± 0.015	4–14	35
с					-0.086 ± 0.013	-0.051 ± 0.013		0-12	95
d			-0.100 ± 0.020		-0.080 ± 0.020	$\begin{array}{c} 0.070 \\ \pm \ 0.020 \end{array}$		0-10	23
e			$+0.002 \\ 0.020$		-0.051	-0.013 0.020		12-18	15
f				-0.047 ± 0.009				0–17	28
g			-0.072 ± 0.006	-0.064 ± 0.009		$^{-0.063}_{\pm 0.006}$		0–12	34
h			-0.111 ± 0.012			-0.079 ± 0.009		0–17	28
i	-0.004 ± 0.005	-0.133 ± 0.002	-0.048 ± 0.017	-0.049 ± 0.017	-0.045 ± 0.017	-0.055 ± 0.017	-0.044 ± 0.030	6-9	3
j				-0.040 ± 0.005				5–15	34
k					-0.039 ± 0.007		-0.045 ± 0.011	0–15	34

a Peimbert et al. (1978), optical spectroscopy, $t^2 = .035$

b Shaver et al. (1983), optical spectroscopy for 30 objects, radio data for 67 objects, $t^2{=}0$

d Simpson et al. (1995), FIR data from KAO, models

e Vilchez & Esteban (1996), long slit optical spectroscopy, $t^2=0$

f Afflerbach et al. (1996), models to reproduce the T_e measured from radio recombination lines in 28 ultracompact H $\rm II$ regions

g Afflerbach et al. (1997), FIR data from KAO: 15 objects + sources from Simpson, models

h Rudolph et al. (1997), FIR data from KAO of 5 H $\scriptstyle\rm II$ regions in the outer Galaxy + results from Simpson models

i Esteban et al. (1999), optical echelle spectroscopy, $t^2 > 0$

j Deharveng et al. (2000), absolute integrated optical fluxes, $t^2=0$, rediscussion of distances

k Martín-Hernández et al. (2002), FIR data from ISO, model grids, rediscussion of distances

TABLE 4. Galactic abundance gradients from H II regions d log(X/H) / dR in kpc⁻¹

30

c Simpson & Rubin (1990), FIR data from IRAS, no icfs

optical data. Actually, what is found is that N^{++}/O^{++} is larger than N^+/O^+ , so it cannot be an ionization correction factor problem. Rubin et al. (1988) suggest that the discrepancy may be due to the neglect of the recombination component of the [O II] $\lambda 3727$ emission. Such an explanation can indeed hold at low T_e (say below 6 000 K) but is not expected to work at high T_e . Another possibility suggested by Rubin et al. (1988) is that the [O III] $\lambda 52 \,\mu$ m and [O III] $\lambda 88 \,\mu$ m lines are optically thick, thus increasing the derived N^{++}/O^{++} . FIR lines from N^{++} and O^{++} have now been observed by ISO (Peeters et al. 2002), but in their analysis Martin-Hernández et al. (2002) do not use them to derive abundance gradients. It is not clear why, since they have constructed photoionization model grids to correct for unseen ions.

The only data on a possible carbon abundance gradient comes from optical recombination lines measures in 3 objects! Obviously more work is needed in this respect.

4.4. The Galactic center

The central parsec of the galaxy, identified with the Sagittarius A nebula, contains ionized gas powered by about 10^{40} ionizing photons sec⁻¹ (Lacy el al. 1980). A cluster of He I emission line stars has been observed and spectroscopically analyzed (Tamblyn et al. 1996, Najarro et al. 1997). The complete spectrum of infrared fine structure lines that has been observed, combined with the H Br α and Br γ lines (see Shields & Ferland 1994 for a compilation) should in principle allow to perform an abundance analysis. From a two-component photoionization model Shields & Ferland (1994) estimate that the abundance of Ar should be about twice solar, but Ne seems rather to have the solar value. The evidence for over solar metallicity is thus mixed. The N/O ratio is estimated to about 3-4 times solar. However, the derived abundances may be clouded by errors in the reddening corrections (the extinction is as high as $A_V=31$, so, even at far infrared wavelengths, reddening become important) and uncertainties in the atomic parameters (mainly those determining the ionization structure). As a consistency check, Shields & Ferland (1994) compared the electron temperature measured from recombination lines with their model predictions. For that, they included heating by dust, and assumed the same grain content as in the model of Baldwin et al. (1991) for Orion. They found the measured temperatures to be consistent with a metallicity 1-2 times solar, while 3 times solar would be only marginally consistent. However, with a population of small grains, photoelectric heating would be more important, and larger metal abundances could be acceptable.

The Galactic center has since then been reobserved by ISO (Lutz et al. 1996), but a detailed discussion of the new results remains to be done.

4.5. Nebulae around evolved massive stars

Evolved massive stars are associated with nebulae which result from the interaction of stellar winds and stellar ejecta with the ambient interstellar medium. By studying the chemical composition of these nebulae, together with their morphology, kinematics and total gas content, one can get insight into the previous evolutionary stages of the stars and unveil some of the nucleosynthesis and mixing processes occuring in their interiors.

Schematically, during main sequence evolution, the fast wind creates a cavity in the interstellar medium and sweeps out a shell of compressed gas. After departure from the main sequence, the nature of the mass loss changes and the star loses chemically enriched material. When the star reaches the Wolf-Rayet phase, its outer layers are almost hydrogen free. This material is lost at high velocity and catches up with material lost in previous stages (see Chu 1991 or Marston 1999 for a review).

Imaging surveys of the environments of WR stars have found that in 50% of cases a

ring like nebula is seen (Marson 1999). Ring nebulae have been classified by Chu (1981) into R type – radiatively excited H II regions and subsonic expansion velocities, E type – nebulae formed out of stellar ejecta (chaotic internal motion, large velocities) and W type – wind-blown bubbles showing thin sheets or filaments. Atlases are published by Chu, Treffers & Kwitter (1983), Miller & Chu (1993) and Marston (1997). Known examples of R types are RCW 78 (amorphous, containing a WN 8 star) and RCW 118 (shell, surrounding a WN 6 star). Known cases of nebulae containing ejecta are M 1-67 (WN 8 star), RCW 58 (WN 8 star). Known W types are NGC 6888 (WN 6 star), S 308 (WN5 star), RCW 104 (WN4 star), although Esteban et al. (1992) consider NGC 6888 as an Bubble/Ejecta type in their classification.

Luminous Blue Variable stars are regarded as precursors of WR stars with the most massive progenitors. They are usually found to be associated with small ejecta type nebulae like η Car, AG Car (Nota et al. 1995).

The first spatially resolved and comprehensive study of abundances in Wolf-Rayet ring nebulae is that of Esteban and coworkers (Esteban et al. 1990, 1991, 1992, 1993, Esteban & Vílchez 1992), in which 11 objects have been analyzed with similar procedures. In a plot relating the N/O and O/H differential abundances (i.e. abundances with respect to interstellar medium ones) Esteban et al. (1992) find that most objects lie close to the $(O/H + N/H) = (O/H + N/H)_{Orion}$ line, indicating that oxygen has been converted into nitrogen. This is indeed what is predicted by the Maeder (1990) stellar evolution models at the beginning of the WN phase. Dividing their objects into 3 categories from their chemical composition (H II for objects with abundances close to those of the environing ISM, DN for diluted nebulae in which stellar ejecta are mixed with ambient gas and SE for pure stellar ejecta), Esteban et al. (1992) show that there is a rather good correspondence between the chemical classes and the morpho-kinematical classes. They also note that the masses of SE nebulae are small and compatible with the hypothesis of pure stellar ejecta, while the H II nebulae have larger dynamic ages, consistent with the idea of being composed of large quantities of swept up gas. Esteban et al. (1992) find that the SE nebulae surrounding WR stars are associated with stars showing variability and thus probably having unstable atmospheres. This is also true for the nebulae associated with LBVs. In plots relating the N/O mass fraction to the He mass fraction, Esteban et al. (1992) find that SE nebulae lie close to the stellar evolution tracks of Maeder (1990) for initial masses $25 - 40 \, M_{\odot}$, which become WN stars after a red supergiant (RSG) phase. This is consistent with the initial masses estimated from the star luminosities (Esteban et al. 1993).

Since this pioneering study, detailed computations have been performed to simulate the evolution of the circumstellar gas around massive stars (García-Segura et al. 1996 a and b), coupling hydrodynamics with stellar evolution. The fate of the circumstellar gas results from interactions between the fast wind from the star while on the main sequence, the slow wind from the red supergiant or luminous blue variable stage and the fast wind from the WR stage. The resulting masses, morphologies and chemical composition of the circumstellar envelopes strongly depend on the initial stellar masses, both because of different nucleosynthesis and different time dependence of the winds. Stars with initial masses around 35 M_{\odot} are predicted to go through a RSG stage, and produce massive nebular envelopes (~ 10 M_{\odot}) with composition only slightly enriched in He and CNO processed material. Stars with initial masses around 60 M_{\odot} are predicted to go through a LBV stage, and produce less massive nebular envelopes (~ 4 M_{\odot}) with helium representing about 70% of the total mass fraction, and CNO equilibrium abundances (C depleted by a factor 23, N enriched by a factor 13, and O depleted by a factor 18). The composition and morphology of NGC 6888 and Sh 308 well agree with the theoretical prediction of a RSG progenitor. On the other hand, Smith (1996) notes that recent abundance determinations in nebulae associated with LBV stars do not agree with the composition predicted by the García-Segura et al. (1996) model of evolution of a 60 M_{\odot} star through the LBV stage. The abundance paterns of these nebulae are rather similar to those of SE nebulae surrounding RSG stars, with mild enrichments in He and N and mild depletion in O, suggesting that the star went through a RSG phase. It must be noted that abundance determinations in such objects are often difficult, because few diagnostic lines are available, so that ratios like N/H or O/H may be rather uncertain, but N/O is more reliable. In a rediscussion of nebulae around LBV stars, Lamers et al. (2001) conclude that the stars have not gone through a RSG phase. The chemical enhancements are due to rotation-induced mixing, and the ejection is possibly triggered by near-critical rotation.

5. Observational results on abundances in planetary nebulae

Until recently, a little less than 20 elements were available for abundance studies in planetary nebulae. These were: H, He, C, N, O, F, Ne, Na, Mg, Si, P, S, Cl, Ar, K, Ca, Mn, Fe, although routine abundance determinations are available for only about 10 elements. As already mentioned and will be made clearer in the next sections, these elements can serve either as probes of the ISM abundances or as probes of the nuclear and mixing processes in the progenitor stars. It has also been mentioned that some elements are heavily depleted in dust grains, so that the abundances of these elements in PNe (Mg, Si, P, K, Ca, Mn, Fe) rather give information on the chemistry of dust grains. This is of great interest since it is now believed that a large portion of grains found in the ISM were actually seeded in the atmospheres of evolved, intermediate mass stars (Dwek 1998).

Recently, ultra deep spectroscopy of bright PNe allowed to detect and measure lines from elements of the fourth, fifth and even sixth row of the Mendeleev table (Péquignot & Baluteau 1994, Baluteau et al. 1995, Dinerstein 2001, Dinerstein & Geballe 2001): V, Cr, Co, Ni, Cu, Zn, Se, Br, Kr, Rb, Sr, Y, Te, I, Xe, Cs, Ba, Pb. When the atomic data for a quantitative analysis of these lines become available (and some atomic physics work has already been fostered by these discoveries, see e.g. Schöning & Butler 1998), this will open a new possibility to test PNe progenitors as production sites of r- and sprocess elements.

The determination of isotopic abundance ratios in PNe would allow serious constraints on the nucleosynthesis in post-AGB stars (see e.g. Forestini & Charbonnel 1997, Marigo 2001). They strongly depend on stellar mass, metallicity and mixing length. Unfortunately, from the observational point of view, this field is still in its infancy. The ${}^{12}C/{}^{13}C$ ratio has been measured in only a couple of nebulae in either hyperfine UV transitions (Clegg et al. 1997, Brage et al. 1998) or in millimetric lines of CO (Bachiller et al. 1997, Palla et al. 2000). The ³He abundance has been determined in a few nebulae from the hyperfine transition at 8.665 GHz (Balser et al. 1997, see also Galli et al. 1997).

5.1. NGC 7027 and IC 418: two test cases

It is instructive to compare the abundances determined by various authors for two bright and well studied PNe.

NGC 7027 is the PN with the highest optical surface brightness despite of 3.5 mag absorption by dust and is a benchmark for PN spectroscopists. It is a very high excitation nebula, with lines of [Ne VI] now measured (Bernard Salas 2001). The central star temperature is estimated to be 140 000 –180 000 K, the gas density is around 5 10^4 cm⁻³.

G. Stasińska: Abundances in H II regions and planetary nebulae

	He	С	Ν	0	Ne	Na	Mg	Si	S	Cl	А	Κ	Ca	Fe
a	10600	600	160	410	100	1.2	22	6.2	9.4	0.11	2.3	.05		
b	11000	955	162	508	137									
с	11100	600	150	300	95	2	50	5	6.9	0.18	2.0	.16	.4	
d	11000	1000	182	436	129		25		10		2.5			1
e		1300	330	420										
f	10000	3000	200	730	220		35		17					
g	10800	2500	275	700	154						18.2			1
h	9120		331	910	275				148	22.4	15.1	.14	.14	

a Bernard Salas et al. (2001), FIR data from ISO + optical + UV, empirical

b Kwitter & Henry (1996), optical + UV data, model

c Keyes et al. (1990), optical + UV data, model

d Middlemass (1990), optical + UV + FIR data, model

e Perinotto et al. (1980), optical + UV data, empirical

f Péquignot et al. (1978), optical + UV + FIR data, model

g Shields (1978), optical + UV + FIR data, model

h Aller 1954, optical data, empirical

TABLE 5. Abundances in NGC 7027

	He	С	Ν	0	Ne	Mg	\mathbf{S}	Cl	Ar
a	90000	219	86	153	9.2				
b	70000	300	70	180	3	6.9	2.5	.1	0.5
с	110000			288	52				2.7
d	72000		66	275	13		3:		0.8
е	93000	616:	74	436	74		4.2	.09	2.3
f		710				25			
g			45	398	19				
\mathbf{h}	> 76000	794	100	760	40				

a Henry et al. (2000), optical + UV data, model

b Hyung et al. (1994), opt echelle + UV + a few IR data, model

c de Freitas Pacheco et al. (1992), optical data, empirical

d Gutierrez Moreno (1988), optical data, empirical

e Aller & Czyzak (1983), optical data, hybrid method

f Harrington et al. (1980), optical + UV data, empirical

g Barker (1978), optical data, empirical

h Torres-Peimbert & Peimbert (1977), optical data, empirical with $t^2 = 0.035$

TABLE 6. Abundances in IC 418

The nebula is surrounded by a dusty neutral shell. Table 5 lists the abundances derived for this object. Substantial differences are seen among the results obtained by various authors. It is interesting to recall that the concommittent models of Shields (1978) and of Péquignot et al. (1978) produced [O II] and [N II] intensities about one order of magnitude smaller than observed. Multidensity geometries and modifications of the stellar continuum failed to resolve this difficulty. Péquignot et al. (1978) postulated

34

the existence of efficient charge transfer processes, and obtained an excellent fit to the observations by adjusting the charge transfer rates. These charge transfer rates were later confirmed by atomic physics computations. In spite of the different approaches adopted by Shields ((1978) and Péquignot et al. (1978), the resulting abundances are rather similar. On the other hand, they are significantly different from the abundances obtained later for this object. This is not only due to the use of different atomic data or to the number and quality of observational constraints (e.g. ISO spectroscopy provided high quality measurements on a large number of IR lines): when models are not entirely satisfactory, the abundances finally adopted are a matter of the author's personal choice.

IC 418 is also a bright and relatively dense $(n \sim 5 \ 10^4 \ \mathrm{cm}^{-3})$ PN, but with a central star of low effective temperature $(T_{\star} \sim 38000 \ \mathrm{K})$, so that fewer ions are observed. The nebula is surrounded by an extended neutral shell. Here again, there are substantial differences among the published abundances. In this case, the differences in O/H cannot be attributed to ionization correction, since O is observed in all its ionization stages. It is actually the observational data which strongly differ from one author to another! Besides, results from empirical methods depend, as we know, on the assumptions made for the temperature structure. As for models, they do not give satisfactory fits for this object and therefore do not provide reliable abundances.

These two examples may serve as a warning that abundances are not necessarily as well determined as might be thought from error bars quoted in the literature.

5.2. What do PN abundances tell us?

The chemical composition of PNe envelopes results from a mixing of elements produced by the central star and dredged up to the surface with the original material out of which the star was made. Basically, the evolution of the central star can be described as follows (Blöcker 1999, Lattanzio & Forestini 1999). After completion of central hydrogen burning through the CNO bicycle, hydrogen burns in a shell around the He core. Due to core contraction the envelope expands. The star evolves towards larger radii and lower effective temperatures and ascends the red giant branch (RGB). During evolution on the RGB, the envelope convection moves downward reaching layers which have previously experienced H-burning (first dredge up), and brings up processed material to the surface. This material is mainly ¹⁴N, ¹³C, ¹²C, and ⁴He (Renzini & Voli 1981).

The ascent on the giant branch is terminated by ignition of the central helium. The subsequent evolution is characterized by helium burning in a convective core and a steadily advancing hydrogen shell. The fusion of helium produces ¹²C by the triple α process, and this carbon is in turn subject to α capture to form ¹⁶O. Eventually the helium supply is totally consumed, leaving a core of carbon and oxygen. The star begins to ascend the giant branch again, now called the asymptotic giant branch (AGB). When a star reaches the AGB, it has the following structure: a CO core, a He burning shell, a He intershell, a H burning shell, and a convective envelope. In stars more massive than 4 M_{\odot}, the envelope penetrates the region where H burning has occured, dredging up some of its material to the stellar surface (second dredge up). During this episode, ¹⁴N and ⁴He increase, while ¹²C and ¹³C decrease with ¹²C/¹³C staying around one, and ¹⁶O slightly decreases.

While on the AGB, the star experiences further nucleosynthesis. Thermal pulses of the He shell induce a flash-driven convection zone, which extends from the helium shell almost to the H shell and deposits there some ¹²C made in the He shell. As the helium flash dies away, the energy deposited causes expansion and cooling, and the external convective region reaches down the carbon-rich region left after the flash, bringing ¹²C and ⁴He to the star surface (third dredge up). During thermal pulses, elements beyond

iron are produced by slow neutron capture (s-process). This requires partial mixing of hydrogen into the carbon rich intershell (Lattanzio & Forestini 1999): these protons are captured by ¹²C to produce ¹³C which later releases neutrons via the ¹³C(α ,n)¹⁶O reaction. For stars above 5 M_{\odot}(at solar metallicity) a second important phenomenon is hot bottom burning. The convective envelope penetrates into the top of the H-burning shell. Temperatures can reach as high as 10⁸ K. This results in the activation of the CN cycle within the envelope, and the consequent processing of ¹²C into ¹³C and ¹⁴N, with the result that ¹²C/¹⁶O is smaller than one.

In summary, nucleosynthesis in PNe progenitors mainly affects the abundances of He, N and C in the envelope. The He abundance increases during the first, second and third dredge up. The ¹⁴N abundance increases during the first, second and third dredge up. In the case of hot bottom burning, primary N is produced out of C synthesized in the He shell and brought to the H shell after the flash. The ¹²C abundance decreases during first and second dredge up but increases during third dredge up, and decreases during hot bottom burning. From the synthetic evolutionary models of Marigo (2001), the resulting enrichment in PNe envelopes with respect to the ISM may be as large as a factor of 10 or more for ¹²C and ¹⁴N.

The abundance of ¹⁶O is slightly reduced as a consequence of hot bottom burning while, as pointed out by Marigo (2001), low mass stars may produce positive yields of ¹⁶O, which is brought to the surface by third dredge up. Globally, the oxygen abundance is expected to be little affected by nucleosynthesis in PN progenitors (Renzini & Voli 1981, Forestini & Charbonnel 1997, van den Hoek & Groenewegen 1997, Marigo 2001). From the synthetic evolutionary models of Marigo (2001), the PN progenitors modify the PN oxygen abundance by at most a factor of 2, the effect being strongest at low metallicities (1/4 solar). At solar and half solar metallicity, the effect is practically negligible. As a consequence, the abundance of oxygen should be representative of the chemical composition of the matter out of which the progenitor star was made. The same holds for the abundances of elements such as Ne, Ar, S. On the other hand, the abundances of He, C, N and the s-process elements tell about the nuclear and mixing processes in the PN progenitors.

When using PNe as indicators of the chemical evolution of galaxies, one should be aware that PNe with different central star masses probe different epochs and are subject to different selection effects. The mere existence of the PN phenomenon requires that the star must have reached a temperature sufficient to ionize the surrounding gas before the ejected envelope has vanished into the interstellar space. Now, the evolution of the central star is more rapid for higher masses. PNe ionized by more massive nuclei reach higher luminosities, and they will be the ones for which abundances will be preferentially measured in distant galaxies. In nearby galaxies and in the Milky Way, observations are feasible for lower luminosity PNe. The observability of a PN depends on the detection threshold, but if it is low enough, PNe with less massive nuclei will be visible for a considerably longer time than PNe with massive nuclei. This results from the post-AGB evolution time being a strongly decreasing function of core mass (see e.g. the models of Blöcker 1995). Another point is that, because of the existence of an initialfinal mass relation (e.g. Weidemann 1987), PNe with less massive nuclei correspond to stars with lower initial masses, which are far more numerous according to the Salpeter initial mass function. For these two reasons, samples of nearby PNe will not contain a large proportion of objects with high mass progenitors. They will not contain many PNe with central star masses below 1–1.5 M_{\odot} either, because such stars are believed to turn into very slowly evolving post-AGB stars and the ejected envelope will have dispersed into the interstellar medium before being ionized. This is why the distribution

progenitor mass	central star mass	progenitor's birth	$PN type^{a}$
$\begin{array}{c} 2.4-8 M_\odot \\ 1.2-2.4 M_\odot \\ 1.0-1.2 M_\odot \\ 0.8-1.0 M_\odot \end{array}$	$\begin{array}{l} > 0.64 \ {\rm M}_\odot \\ 0.58 - 0.64 \ {\rm M}_\odot \\ \sim 0.56 \ {\rm M}_\odot \\ \sim 0.555 \ {\rm M}_\odot \end{array}$	1 Gyr ago 3 Gyr ago 6 Gyr ago 10 Gyr ago	Type I Type II Type III Type IV
^{<i>a</i>} PN types accord	ding to Peimbert (197	8, 1990)	

TABLE 7. Schematical classification of PNe and their progenitors

of central star masses is so strongly peaked around 0.6 M_{\odot} (Stasińska et al. 1997). PNe of different central star masses probe different epochs of galaxy history. Schematically, they can be classified as shown in Table 7 (which however must be taken only as a rough guideline). The subdivision of PNe into four types by Peimbert (1978) was motivated by this kind of considerations (but several revisions to his initial scheme were proposed later, as will be discussed in Sect. 5.4.1). All the above considerations need confirmation from observational data on PNe samples.

5.3. PNe as probes of the chemical evolution of galaxies

5.3.1. The universal Ne/H versus O/H relation

From a compilation of PNe abundances in the Galaxy and in the Magellanic Clouds, Henry (1989) found that the Ne/H versus O/H relation for PNe is very narrow and linear in logarithm. It is also identical to the one found for H II regions (Vigroux et al. 1987). This implies that Ne and O abundances in intermediate mass stars are not significantly altered by dredge up, and therefore that oxygen and neon abundances in PNe can indeed be used to probe the interstellar abundances of oxygen over a large portion of the history of galaxies.

5.3.2. Abundance gradients from PNe in the Milky Way

Table 8 presents a compilation of Galactic abundance gradients from PNe in units of d $\log(X/H) / dR$ in kpc⁻¹. Column 9 shows the spanned range of galactocentric distances in kpc. Column 10 gives the total number of objects used to derive the gradients. Note that, as in the case of H II regions, the quoted uncertainties in the published abundance gradients include only the scatter in the nominal values of the derived abundances. In the case of PNe, distances are not known with good accuracy, they are usually derived from statistical methods, typically within a factor of 2 or more. However, if a gradient is found with erroneous distances, this means that a gradient is indeed most likely present, since one does not expect a conspiration of errors in distances to produce a spurious gradient. On the other hand, the values of the computed gradient strongly depend on the adopted PNe distance scale, as noted by Amnuel (1993). Only PNe arising from disk population stars are suitable to determine abundance gradients in the Galactic disk. Therefore, high velocity PNe (Type III according to the classification by Peimbert 1978) and a fortiori PNe belonging to the halo (Type IV PNe) are not suitable for this purpose.

It is to be noted that, while the existence of gradients seems established, there are significant differences in the magnitudes of these gradients as found by different authors. At present, it is not possible to say how accurate these gradients are. Note that account-

	Не	С	Ν	0	Ne	S	Ar	range	nb
a				054 ± .019				5-12	43
b					$036 \pm .010$			4-14	128
с					$056 \pm .007$			4-13	91
d	009 ± .01			03 ± .01				1-14	277
e	004 ± .003				$^{030}_{\pm .012}$				74
f	023 ± .0033			031 ± .0199		$082 \pm .027$		1-11	15
g	011 ± 0.003			$^{014}_{\pm .016}$				1-9	21
h	019 ± .003			$.072 \pm .012$		098 ± .022		7-14	42

a Martins & Viegas (2000), Type II, homogeneous rederivation of abundances from compiled intensities

b Maciel & Quireza (1999), Type II, abundances compiled from the literature

c Maciel & Koppen (1994), Type II, abundances compiled from the literature

d Pasquali & Perinotto (1993), Type I + II , abundances compiled from the literature e Amnuel (1993), Type In (according to his classification), abondances compiled from the literature

f Samland & al. (1992), Type II, homogeneous observational material an automated photoionization model fitting

g Köppen & al. (1991), Type II, homogeneous observational material and empirical abundance derivations

h Faundez-Abans & Maciel (1983), Type II, abundances compiled from the literature.

TABLE 8. Galactic abundance gradients from PNe d log(X/H) / dR in kpc⁻¹

ing for possible "temperature fluctuations" would probably steepen the derived gradients (Martins & Viegas 2000).

From the most recent results, galactic gradients found for O, Ne and S using PNe appear to be similar to the ones found from H II regions and young stars (Maciel & Quireza 1999). This suggests that abundance gradients in the Galaxy have not changed during the last 3 Gyr. N and C gradients are different between PN and H II regions, which is expected of course. Their values have been reported in Table 8 only to be complete, but the existence of N or C gradients in PNe populations would rather tell

38

ref	He	Ν	0	Ne	S	Ar	nb
a		$\begin{array}{c} 8.13 \\ \pm \ 0.42 \end{array}$	$\begin{array}{c} 8.48 \\ \pm \ 0.43 \end{array}$	$\begin{array}{c} 7.96 \\ \pm \ .36 \end{array}$			85
b		$\begin{array}{c} 8.12 \\ \pm \ 0.37 \end{array}$	$\begin{array}{c} 8.74 \\ \pm \ 0.15 \end{array}$			$\begin{array}{c} 6.28 \\ \pm \ 0.37 \end{array}$	30
с	$.126 \pm .027$		$\begin{array}{c} 8.22 \\ \pm \ 0.43 \end{array}$		$\begin{array}{c} 6.48 \\ \pm \ 0.93 \end{array}$	$\begin{array}{c} 5.95 \\ \pm \ 0.55 \end{array}$	45

a Stasińska et al. (1998), compiled intensities, homogeneous abundance derivations b Cuisinier et al. (2000), homogeneous data, results kindly provided by A. Escudero c Escudero & Costa (2001), homogeneous data

TABLE 9. Mean abundances of PNe in the Galactic bulge

something on the stellar populations from which the PN arise. As for the C gradients, they are highly unreliable anyway.

We can compare the average O/H in PNe and in H II regions of the solar vicinity, using the gradients given in Tables 4 and 8 and adopting for simplicity that the galactocentric distance of the Sun is 8.5 kpc. We find that $12+\log O/H = 8.81 \pm 0.04$ using the H II regions data from Shaver et al. (1983), 8.606 ± 0.06 using those from Afflerbach et al. (1997), and 8.63 ± 0.05 using Type II PNe from the compilation of Maciel & Quireza (1999). There is therefore no compelling evidence that O/H differs between Type II PNe and H II regions in the solar vicinity. This is a further indication that ISM abundances have remained constant during the last few Gyr and that there is no significant modification of O/H in PNe due to mixing in the progenitors.

Maciel & Köppen (1994) have examined whether abundance gradients in the Galaxy steepen with time, by comparing the gradients from Type I, Type II and Type III PNe. The evidence is marginal.

The question of possible vertical abundance gradients has been investigated by Faundez-Abans & Maciel (1988), Cuisinier et al. (1996) and Köppen & Cuisinier (1997), the latter study being the most detailed. Adopting careful selection criteria on the quality of the spectra and the location of the PNe in the Galaxy in a sample of 94 PNe, the latter authors find a systematic decrease of the abundances of He, N, O, S and Ar with height above the plane. The N/O ratio also exhibits a clear decrease with height. These findings are compatible with a simple empirical model that the authors work out for the kinematical and chemical evolution of the solar neighbourhood in which the progenitor stars are supposed to be born in the galactic plane and reach greater heights due to the velocity dispersion that increases with age.

5.3.3. PNe in the Galactic bulge

Planetary nebulae offer one the best means to investigate the oxygen abundance in the Galactic bulge. Table 9 presents the mean oxygen abundances for PNe thought to be physically located in the Galactic bulge, using recent data. In all cases, the abundance derivations were made with T_e -based methods. The abundances derived by Ratag et al. (1997) have not been included, since many of them rely on modelling of objects with no observed constraint of T_e , and are therefore highly suspect (see discussion in Sect. 2.2.1).

	He	Ν	0	Ne	S	Ar
a		8.86	9.16	8.51	7.83	
		± 0.29	± 0.16	± 0.30	± 0.30	
b			9.13	8.29	7.52	6.79
			$\pm .05$	$\pm .08$	$\pm .08$	$\pm .08$
с			9.25	8.46	7.46	7.07
			± 0.05	± 0.06	± 0.05	± 0.07
f	10.91	7.74	8.73		6.83	6.22
	± 0.014	± 0.22	± 0.09		± 0.13	± 0.10
g			8.81		6.89	6.39
			$\pm .08$		± 0.12	± 0.05
	Martins &					
c l	Maciel & Q Maciel & K	öppen (19				
	Samland & Köppen & a					

TABLE 10. Abundances at the galactic center extrapolated from disk PNe

However, the observations from Ratag et al. (1997) were used in the compilation of line intensities by Stasińska et al. (1998), and the abundances rederived in a consistent way with T_e -based methods (for objects for which this was possible). The objects of Escudero & Costa (2001) are newly discovered PNe from the list of Beaulieu et al. (1999). We see that the abundances of PNe in the Galactic bulge have clearly higher mean values and dispersions in O/H than the extrapolation from disk PNe towards the Galactic center, which are shown in Table 10. The effect may be even stronger than suggested from these tables, since samples of PNe considered as belonging to the Galactic bulge may actually contain PNe of the disk population that are found physically in the same region as the bulge.

Combining data on about 100 PNe in the Galactic bulge from the works of Cuisinier et al. (2000), Webster (1988), Aller & Keyes (1987) with their own data, Escudero & Costa (2001) suggest the existence of a vertical abundance gradient in the bulge, with lower O/H at high latitudes.

5.3.4. PNe in the Galactic halo

Only a small number of PNe in the halo are known so far, less than 20, for an expected total of several thousands (see e.g. Tovmassian et al. 2001). This number is however rapidly growing, thanks to systematic sky surveys at high Galactic latitudes for the search of emission line galaxies, and in which PNe are discovered serendipitously. Halo PNe belong to an old metal poor stellar population, and therefore serve as probes of the halo chemical composition at the time of the formation of their progenitors. They also give the opportunity to study mixing processes in metal poor intermediate mass stars.

Using published spectral line data, Howard et al. (1997) rederived the chemical com-

position of 9 halo PNe in a consistent way. They found that all had subsolar O/H, the most oxygen poor being K648, with log O/H + 12=7.61 (i.e. about 1/20 of the Anders & Grevesse 1989 solar value). They also found that the spread in Ne/O, S/O and Ar/O is much larger than can be accounted for by uncertainties alone. This scatter in PNe abundances is similar to the scatter observed in halo stars (Krishnaswamy-Gilroy et al. 1988), and suggests that accretion of extragalactic material occured during formation of the halo. It must be noted however that, among PNe considered to be in the halo, some actually probably belong to an old disk population (Torres-Peimbert et al. 1990).

After the study of Howard et al. (1997), a few other PNe were discovered in the halo and their chemical composition analyzed (Jacoby et al. 1997, Napiwotzki et al. 1994, Tovmassian et al. 2001). The most spectacular one is SBS 1150+599A (renamed PN G 135.9+55.9), which has an oxygen abundance less than 1/100 solar (Tovmassian et al. 2001). This makes it by far the most oxygen poor PN known (and perhaps the most oxygen poor *star* known). One may ask whether the oxygen abundance in this object really reflects that of the initial star. Indeed, bright giants in metal poor globular clusters seem to present star to star oxygen abundance variations (see e.g. Ivans et al. 1999), and mixing processes have been invoked to explain these abundance patterns (see Charbonnel & Palacios 2001 for a review). One could invoke that a similar process affects the oxygen abundance in PN G 135.9+55.9. However, Ne is found to be also strongly underabundant in this object (Ne/O ~ 0.3, paper in preparation), indicating that this object is indeed extremely metal poor. In that case, the progenitor must have formed very early in the Galaxy but given rise to a PN only recently. Alternatively, it could have formed out of infalling metal poor material at a more recent epoch.

5.3.5. PNe probe the histories of nearby galaxies

A wealth of data exist for large samples of PNe in the Magellanic Clouds, both in the optical and in the UV (Monk et al. 1988, Boroson & Liebert 1989, Meatheringham & Dopita 1991 a, b, Vassiliadis et al. 1992, Leisy & Dennefeld 1996, Vassiliadis et al. 1996, 1998). PNe in the Magellanic Clouds represent a statistically significant sample at a common distance, suffering little extinction along the line of sight, and sufficiently bright to allow the measurement of diagnostic lines from various ions.

The oxygen abundances of PNe in the Magellanic Clouds span a relatively small range: log O/H + 12 = 8.10 ± 0.25 from a compilation of 125 objects for the LMC, log O/H + 12 = 7.74 ± 0.39 from a compilation of 48 objects for the SMC reanalyzed in a homogeneous way by Stasińska et al. (1998). If one considers only the high luminosity sample ($L_{\rm [O~III]}$ > 100 L_{\odot}), the spread is smaller and the mean abundance is significantly larger: 8.28 ± 0.13 (40 objects) for the LMC, 8.09 ± 0.11 (11 objects) for the SMC. This has been interpreted as due to the fact that, as a class, high luminosity PNe have progenitors of higher masses, therefore younger and made of more chemically enriched gas. The mean oxygen abundance in the high luminosity class compares well with that from H II regions in the Magellanic Clouds: 8.35 ± 0.06 for LMC, 8.03 ± 0.10 for SMC (Russell & Dopita 1992). This indicates that the oxygen abundance in luminous PNe is a very good proxy of the present day ISM oxygen abundances.

Dopita et al. (1997) have produced self consistent photoionization models to fit the observed line fluxes between 1200 and 1800 Å for 8 PNe in the LMC. With these models they obtain not only the elemental abundances, but also the temperatures and luminosities of the central stars. This allows them to place the objects in the HR diagram and derive the central star masses and post-AGB evolution times by comparison with theoretical tracks for post-AGB stars of various masses (the choice of H-burning or He-burning track for each object is made by the requirement of consistency with the observed expan-

42 G. Stasińska: Abundances in H II regions and planetary nebulae

sion age of the nebula). Assuming the initial-final mass relation of Marigo et al. (1996), Dopita et al. (1997) are able to estimate the masses of the progenitors. This allows them to trace the age-metallicity relationship in the LMC. As a proxy of metallicity, they use the sum of the abundances from the α -process elements Ne, S, Ar (in order to alleviate any doubts that might come from the use of O whose abundance can be slightly affected by mixing processes). They find that the LMC experienced a long period of quiescence, followed by a short period activity within the past 3 Gyr which multiplied its metallicity by a factor 2. A further study is under way by the same autors to include 20 additional PNe in the LMC and 10 PNe in the SMC.

PN spectroscopy is now possible with relatively high signal-to-noise even in more distant galaxies. For example, observations of 28 PNe in the bulge of M31 and 9 PNe in the companion dwarf galaxy M32 allowed to obtain T_e -based abundances for these objects (Richer et al. 1999). The oxygen abundances of the PNe observed in the bulge of M31 are found to be very similar to those of the luminous PNe in the Galactic bulge (the comparison, in order to be meaningful, must be done on nebulae with similar luminosities, since the oxygen abundances has been shown to depend on luminosity in the Magellanic Clouds and the Galactic bulge). One finds $\log O/H + 12 = 8.64 \pm 0.23$ for the M31 bulge sample and 8.67 ± 0.21 for the high luminosity PNe in the Galactic bulge (Stasińska et al. 1998). Jacoby & Ciardullo (1999) obtained spectroscopic data on 12 PNe in the bulge and 3 in the disk of M31. They span a larger luminosity range than Richer et al. (1999) who were mainly interested in bright PNe. For the three objects in common with Richer et al. (1999), the oxygen abundances are in excellent agreement. Yet, for their entire sample, Jacoby & Ciardullo (1999) find log O/H + $12 = 8.50 \pm 0.23$ which is significantly lower than the value found by Stasińska et al. (1998), possibly because of the larger range of PNe luminosities in their sample.

The data on M32 by Richer et al. (1999) confirm the suggestion by Ford (1983) that the PNe in M32 are nitrogen rich. It seems unlikely that all the luminous PNe have high enough central star masses to undergo second dredge up, and this finding suggests that in M32 nitrogen was already enhanced in the precursor stars.

Other local group galaxies have smaller masses and therefore contain only a few PNe. Abundance data exist for PNe in NGC 6822, NGC 205, NGC 185, Sgr B2, Fornax (see references in Richer & Mc Call 1995 and Richer et al. 1998).

Richer & Mc Call (1995) compared the oxygen abundances from PNe in diffuse ellipticals and dwarf irregulars. They found that diffuse ellipticals have higher abundances than similarly luminous dwarf irregulars. This seems consistent with the idea that diffuse ellipticals would be the faded remnants of dwarf ellipticals. However, when considering also the O/Fe ratios, obtained by combining stellar abundance measurements, they conclude that diffuse ellipticals and dwarf ellipticals have had in fact fundamentally different star formation histories.

Combining the data on PNe in these dwarf spheroidals galaxies with those on PNe in M32 and in the bulge M31 and of the Milky Way, Richer et al. (1998) have shown that the mean oxygen abundance correlates very well with the mean velocity dispersion. Since the oxygen abundance of luminous PNe is a good proxy of the oxygen abundance in the ISM at the time when star formation stopped, this implies that there is a correlation between the energy input from supernovae and the gravitational potential energy. Such a correlation arises naturally if chemical evolution in these systems is stopped by Galactic winds.

The oxygen abundances found in the elliptical galaxy NGC 5128 (Centaurus-A) by Walsh et al. (1999) show a mean value of about 8.4, i.e. smaller than the mean value determined for the bright PNe in M31. This result is somewhat difficult to understand for such a massive galaxy, unless the most metal rich stars do not produce observable PNe. This possibility is known as the the AGB manqué phenomenon (see e.g. Greggio & Renzini 1990), by which intermediate mass stars do not reach the top of the AGB due to intense stellar winds.

5.4. PNe probe the nucleosynthesis in their progenitor stars

5.4.1. Global abundance ratios

It is clear from the diagrams presented by Henry et al. (2000) that PNe show significantly higher values of He/H, N/O, C/O than H II regions of the same O/H. This indicates that He, N and C have been synthesized in PNe progenitors, as theory predicts. More quantitative comparison with theory is difficult because of the number of determining parameters (stellar mass, parametrization of the mixing processes) and of complex selection effects. In the following we draw a few examples of more detailed interpretations of abundance ratios that have been proposed.

The nature of Type I PNe is a good example of the difficulty in the interpretation. Peimbert (1978) had defined type I PNe as objects having He/H > 0.125 and N/O >0.5. Kaler et al. (1978) interpreted the high N/O and He/H together with the (He/H, N/O correlation observed in such objects as due to second dredge up, implying initial stellar masses larger than 3 M_{\odot}. Later, the He/H criterion to define Type I PNe was abandoned (it must be noted that old determinations of He/H did not include proper correction for collisional excitation of He lines). Henry (1990) found that Type I PNe showed an (N/O, O/H) anticorrelation and concluded that in these objects N is produced at the expense of O (due to ON cycling). Kingsburgh & Barlow (1994) contested the existence of such an anticorrelation and propose a new definition of Type I PNe, as being PNe that underwent envelope burning conversion to N of dredged up primary C. Thus they are objects in which the present N/H is larger than the initial (C+N)/H (equal to 0.8 in the solar vicinity). Costa et al. (2000) on the contrary define Type I PNe using only the criterion He/H > 0.11. They find a (N/O, O/H) anticorrelation when PNe are segregated by types. They interpret this by saving that the oxygen abundance is not modified by the PN progenitor but reflects the metallicity of the site where the progenitor was born, and that dredge-up is more efficient at low metallicity. It must be noted that, whatever the definition, there is actually no clear dichotomy between Type I and other PNe, the distribution of the N/O ratios is rather continuous (and this is also what is predicted at least at solar and half solar metallicities from the models of Marigo 2001).

Concerning carbon, (C+N+O)/H is found to increase with C/H and becomes dominated by C/H for the most carbon rich objects. This is seen both in Galactic samples (Kingsburgh & Barlow 1994) and in Magellanic Clouds samples (Leisy & Dennefeld 1996). This is in agreement with a scenario where carbon is produced by $3-\alpha$ from He and brought to the surface by third dredge up. From the number of PNe with observed C enhancement, one concludes that third dredge up is common in PNe progenitors. Among the PNe in which the carbon abundance could be determined, about 40% (in the Galactic sample) and 70% (in the Magellanic Clouds sample) have C/O > 1. This is well in line with theoretical predictions that third dredge up is more efficient at low metallicity. Note that PNe with C/O > 1, the so-called carbon-rich PNe, are likely to contain carbon rich dust, since their progenitors must have developed a carbon chemistry to form grains in their atmospheres.

More detailed comparisons of PNe results with the predictions of post AGB models have been attempted by Henry et al. (2000) and Marigo (2001). Interpretations are difficult, due to the number of parameters involved and to the difficulty to derive accurate central star masses and to relate them to initial masses.

44 G. Stasińska: Abundances in H II regions and planetary nebulae

Péquignot et al. (2000) discuss two PNe in the Sgr B2 galaxy, He 2-436 and Wray 16-423, whose nuclei are interpreted as belonging to the same evolutionary track. The authors perform a differential analysis of these two PNe, based on tailored photoionization modelling, and argue that while systematic errors may substantially shift the derived abundances, the conclusions based on *differences* between the two models should not be influenced. The main conclusion is that third dredge up O enrichment is observed in He 2-436, at the 10 % level.

5.4.2. Abundance inhomogeneities

Many studies have suggested that structures seen in planetary nebulae (extended haloes, condensations) have different composition from the main nebular body, indicating that they are formed of material arising in distinct mass loss episodes characterized by different chemical compositions of the stellar winds. However, these differences in chemical composition may be spurious, due inadequacies of the adopted abundance determination scheme. For example, the knots and other small scale structures seen in PNe are possibly the result of instabilities or magnetic field shaping, and their spectroscopic signature could be due to a difference in the excitation conditions and not in the chemical composition. In the following, some examples of such studies are presented, adopting the view of their authors.

a) Extended haloes

NGC 6720, the "ring nebula" is surrounded by two haloes: an inner one, with petallike morphology, and an outer one, perfectly circular, as seen in the pictures of Balick et al. (1992). Guerrero et al. (1997) have studied the chemical composition of these haloes, and found that the inner and outer halo seem to have same composition, suggesting a common origin: the red giant wind. On the other hand, the N/O ratio is larger in the main nebula by a factor of 2, indicating that the main nebula consists of superwind and the haloes of remnants of red giant wind.

NGC 6543, the "cat eye nebula" also shows two halo structures: an inner one, consisting of perfectly circular rings, and an outer one with flocculi attributed to instabilities (Balick et al. 1992). Unlike what is advocated for NGC 6720, the rings and the core in NGC 6543 seem to have same chemical composition (Balick et al. 2001). It must be noted however, that the abundances may not be reliable, since a photoionization model for the core of NGC 6543 predicts a far too high [O III] λ 4363/5007 (Hyung et al. 2000). Another puzzle is the information provided by *Chandra*. Chu et al. (2001) estimated that the abundances in the X-ray emitting gas are similar to those of the fast stellar wind and larger than the nebular ones. On the other hand, the temperature of the X-ray gas (~ 1.7 10⁶ K) is lower by two orders of magnitudes than the expected post shock temperature of the fast stellar wind. This would suggest that the X-ray emitting gas is dominated by nebular material. These findings are however based on a crude analysis and more detailed model fitting is necessary.

b) FLIERs and other microstructures

A large number of studies have been devoted to microstructures in PNe, and their nature is still debated. Fast Low Ionization Emission Regions (FLIERs) have first been considered to show an enhancement of N and were interpreted as being recently expelled from the star (Balick et al. 1994). However, Alexander & Balick (1997) realized that the use of traditional ionization correction factors may lead to specious abundances. Dopita (1997) made the point that enhancement of [N II] $\lambda 6584/H\alpha$ can be produced by shock compression and does not necessarily involve an increase of the nitrogen abundance. Gonçalves et al. (2001) have summarized data on the 50 PNe known to have low ionization structures (which they call LIS) and presented a detailed comparison of model predictions with the observational properties. They conclude that not all cases can be satisfactorily explained by existing models.

c) Cometary knots

The famous cometary knots of the Helix nebula NGC 7293 have been recently studied by O'Dell et al. (2000) using spectra and images obtained with the HST. The [N II] $\lambda 6584/H\alpha$ and [O III] $\lambda 5007/H\alpha$ ratios were shown to decrease with distance to the star. Two possible interpretations were offered. Either this could be the consequence of a larger electron temperature close to the star due to harder radiation field. Or the knots close to the star would be more metal-rich, in which case they could be relics of blobs ejected during the AGB stage rather than formed during PN evolution. Obviously, a more thorough discussion is needed, including a detailed modelling to reproduce the observations before any conclusion can be drawn.

d) Planetary nebulae with Wolf-Rayet central stars

About 8% of PNe possess a central star having Wolf-Rayet characteristics, with H-poor and C-rich atmospheres. The evolutionary status of these objects is still in question. A late helium flash giving rise to a "born-again" planetary nebula, following a scenario proposed by Iben et al. (1983), can explain only a small fraction of them. The majority appear to form an evolutionary sequence from late to early Wolf-Rayet types, starting from the AGB (Górny & Tylenda 2000, Peñ at et al. 2001). This seemed in contradiction with theory which predicted that departure from the AGB during a late thermal pulse does not produce H-deficient stars. Recently however, it has been shown that convective overshooting can produce a very efficient dredge up, and models including this process are now able to produce H-deficient post-ABG stars following a thermal pulse on the AGB (Herwig 2000, 2001, see also Blöcker et al. 2001). It still remains to explain why late type Wolf-Rayet central stars seem to have atmospheres richer in carbon than early type ones (Leuenhagen & Hamann 1998, Koesterke 2001). Also, one would expect the chemical composition of PNe with Wolf-Rayet central stars to be different from that of the rest of PNe. This does not seem to be the case, as found by Górny & Stasińska (1995), basing on a compilation of published abundances: PNe with Wolf-Rayet central stars are indistinguishable from other PNe in all respects except for their larger expansion velocities. Peña et al. (2001) obtained a homogeneous set of high spectral resolution optical spectra of about 30 PNe with Wolf-Rayet central stars and reached a similar conclusion, as far as He and N abundances are concerned. Their data did not allow to draw any conclusion as regards the C abundances.

e) H-poor PNe

There are only a few PNe which show the presence of material processed in the stellar interior. They are referred to as H-poor PNe, although the H-poor material is actually embedded in an H-rich tenuous envelope. The two best known cases are A 30 and A 78, whose knots are bright in [O III] λ 5007 and He II λ 4686 but in which Jacoby (1979) could not detect the presence of H Balmer lines. With deeper spectra, Jacoby & Ford (1983) estimated the He/H ratio to be ~ 8 in these two objects. Harrington & Feibelman (1984) obtained IUE spectra of a knot in A 30, and found that the high C/He abundance implied by C II λ 4267 is not apparent in the UV spectra, suggesting that the knot contains a cool C-rich core. Guerrero & Manchado (1996) obtained spectra of the diffuse nebular body of A30, showing it to be H-rich. A similar conclusion was obtained by Manchado et al. (1988) and Medina & Peña (1999) for the outer shell of A 78. However, quantitatively, the results obtained by these two sets of authors are quite different and a deeper analysis is called for.

Three other objects belong to this group: A 58, IRAS1514-5258 and IRAS 18333-2357, the PN in the globular cluster M22, already mentioned in Sect. 3.7.5.

46 G. Stasińska: Abundances in H II regions and planetary nebulae

One common characteristic of this class of objects is their extremely high dust to gas ratio, and the fact that the photoelectric effect on the grains provides an important (and sometimes dominant) contribution to the heating of the nebular gas (see Harrington 1996). This may lead to large point-to-point temperature variations (see Sect. 3.7.5) and strongly affect abundance determinations.

Harrington (1996) concludes his review on H-poor PNe by noting that the H-poor ejecta cannot be explained by merely taking material with typical nebular abundances and converting all H to He. There is additional enrichment of C, N, perhaps O, and most interestingly, of Ne. However, more work on these objects is needed – and under way (e.g. Harrington et al. 1997) – before the abundances can be considered reliable. Stellar atmosphere analysis of H-deficient central stars (e.g. Werner 2001) is providing complementary clues to the nature and evolution of these objects.

In conclusion, we have shown how nebulae can provide powerful tools to investigate the evolution of stars and to probe the chemical evolution of galaxies. Nevertheless, is necessary to keep in mind the uncertainties and biases involved in the process of nebular abundance derivation. These are not always easy to make out, especially for the non specialist. One of the aims of this review was to help in maintaining a critical eye on the numerous and outstanding achievements of nebular Astronomy.

ACKNOWLEDGMENTS: It is a pleasure to thank the organizers of the XIII Canary Islands Winterschool, and especially César Esteban, for having given me the opportunity to share my experience on abundance determinations in nebulae. I also wish to thank the participants, for their attention and friendship. I am grateful to Miriam Peña, Luc Jamet and Yuri Izotov for a detailed reading of this manuscript, to Daniel Schaerer for having provided useful information on stellar atmospheres and to André Escudero for having kindly computed a few quantities related to planetary nebulae in the galactic bulge. I would like to thank my collaborators and friends, especially Rosa González Delgado, Slawomir Górny, Claus Leitherer, Miriam Peña, Michael Richer, Daniel Schaerer, Laerte Sodré, Ryszard Szczerba and Romuald Tylenda for numerous and lively discussions in various parts of the World.

Finally, I would like acknowledge the possibility of a systematic use of the NASA ADS Astronomy Abstract Service during the preparation of these lectures.

REFERENCES

Aanestad, P. A., 1989, ApJ, 338, 162

Afflerbach, A., Churchwell, E., Acord, J.M., Hofner, P., Kurtz, S., Depree, C.G., 1996, ApJS, 106, 423

Afflerbach, A., Churchwell, E., Werner, M.W., 1997, ApJ, 478, 190

Alexander, J., Balick, B., 1997, AJ, 114, 713

AllendePrieto, C., Lambert, D.L., Asplund, M., 2001, ApJ, 556, L63

Aller, L.H., 1942, ApJ, 95, 52

Aller, L.H., 1954, ApJ, 120, 401

Aller, L. H., 1984, Physics of thermal gaseous nebulae, Reidel, Dordrecht

Aller, L.H., Czyzak, S.J., 1983, ApJS, 51, 211

Aller, L.H., Keyes, C.D., 1987, ApJS, 65, 405

Alloin, D., Collin-Souffrin, S., Joly, M., Vigroux, L., 1979, A&A, .78, 200

Amnuel, P.R, 1993, MNRAS.261, 263

Anders, E., Grevesse, N., 1989, GeCoA, 53, 197

Bachiller, R., Forveille, T., Huggins, P.J., Cox, P., 1997, A&A, 324.1123

- Baldwin,J.A., Crotts,A., Dufour,R.J., Ferland,G.J., Heathcote,S., Hester,J.J., Korista,K.T., Martin,P.G., O'dell,C.R., Rubin,R.H., Tielens,A.G.G.M., Verner,D.A., Verner,E.M., 1996, ApJ, 468, L115
- Baldwin, J.A., Ferland, G.J., Martin, P.G., Corbin, M.R., Cota, S.A., Peterson, B.M., Slettebak, A. 1991, ApJ, 374, 580
- Balick, B., Gammon, R.H., Hjellming, R.M., 1974, PASP, 86, 616
- Balick, B., Gonzalez, G., Frank, A., Jacoby, G., 1992, ApJ, 392, 582
- Balick, B., Perinotto, M., Maccioni, A., Terzian, Y., Hajian, A., 1994, ApJ, 424, 800
- Balick, B., Wilson, J., Hajian, A. R., 2001, ApJ, 121, 354
- Balser, D. S., Bania, T.M., Rood, R.T., Wilson, T.L., 1997, ApJ, 483, 320
- Baluteau, J.-P., Zavagno, A., Morisset, C., Péquignot, D., 1995, A&A, 303, 175
- Barbaro, G., Mazzei, P., Morbidelli, L., Patriarchi, P., Perinotto, M., 2001, A&A, 365, 157
- Barker, T., 1978, ApJ, 220, 193
- Barlow, M.J.1993, in Planetary nebulae, IAU Symposium no. 155, Eds. R. Weinberger and A. Acker, Kluwer Academic Publishers, Dordrecht, p.163
- Bautista, M. A., Kallman, T. R., 2001, ApJS 134, 139
- Bautista, M.A., Pogge, R.W., Depoy, D.L., 1995, ApJ, 452, 685
- Bautista, M.A., Pradhan, A.K., 1998, ApJ, 492, 650
- Bautista, M.A., Pradhan, A.K., Osterbrock, Donald E., 1994, ApJ, 432, L135
- Beaulieu, S.F., Dopita, M.A., Freeman, K.C., 1999, ApJ, 515, 610
- Benjamin, R.A., Skillman, E.D., Smits, D.P., 1999, ApJ, 514, 307
- BernardSalas, J., Pottasch, S.R., Beintema, D.A., Wesselius, P.R., 2001, A&A, 367, 949
- Binette, L., Luridiana, V., Henney, W.J, 2001, RMxAC, 10, 19
- Blöcker, T., 1995, A&A, 299, 755
- Blöcker, T., 1999, in Asymptotic Giant Branch Stars, IAU Symposium no. 191, Ed. T. Le Bertre, A. Lèbre, & C. Waelkens, p. 21
- Blöcker, T., T., Osterbart, R., Weigelt, G., Balega, Y., Men'shchikov, A., 2001, in Post-AGB Objects as a Phase of Stellar Evolution, Eds. R. Szczerba & S. K. Górny, Kluwer, p. 241
- Borkowski, K.J., Harrington, J.P., 1991, ApJ, 379, 168
- Boroson, T.A., Liebert, J., 1989, ApJ, 339, 844
- Brage,T., Judge,P.G., Aboussaid,A., Godefroid,M.R., Joensson,P., Ynnerman,A., Froese Fischer,C., Leckrone,D.S., 1998, ApJ, 500, 507
- Butler, K., 1993, in Planetary nebulae, IAU Symposium no. 155, Eds. R. Weinberger and A. Acker, Kluwer Academic Publishers, Dordrecht, p.73
- Caplan, J., Deharveng, L., Peña, M., Costero, R., Blondel, C., 2000, MNRAS, 311, 317
- Cardelli, J.A., Clayton, G.C., Mathis, J.S., 1989, ApJ, 345, 245
- Cardelli, J.A., Meyer, D.M., Jura, M., Savage, B.D., 1996, ApJ, 467, 334
- Casassus, S., Roche, P. F., Barlow, M. J., 2000, MNRAS, 314, 657
- Charbonnel, C., Palacios, A., 2001, Ap&SS, 277, 157
- Chu, Y.-H., 1981, ApJ, 249, 195
- Chu,Y.-H., 1991, in Wolf-Rayet Stars and Interrelations with Other Massive Stars in Galaxies, IAU Symposium no. 143, Ed. K. A. van der Hucht and B. Hidayat, Kluwer Academic Publishers, Dordrecht, p. 349
- Chu,Y.-H., Guerrero,M.A., Gruendl,R.A., Williams,R.M., Kaler,J.B., 2001, ApJ, 553, L69
- Chu, Y.-H., Treffers, R.R., Kwitter, K.B., 1983, ApJS, 53, 937
- Clegg, R.E.S., Harrington, J.P., Barlow, M.J., Walsh, J.R., 1987, ApJ, 314, 551

Clegg, R.E.S., Storey, P.J., Walsh, J.R., Neale, L., 1997, MNRAS, 284, 348

- G. Stasińska: Abundances in H II regions and planetary nebulae
- Cohen, M., Harrington, J.P., Hess, R., 1984, ApJ, 283, 687
- Cota,S.A., Ferland,G.J.,1988, ApJ, 326, 889

48

- Cuisinier, F., Acker, A., Köppen, J., 1996, A&A, 307, 215
- Cuisinier, F., Maciel, W.J., Köppen, J., Acker, A., Stenholm, B., 2000, A&A, 353, 543
- Cunha,K., Lambert,D.L.,1994, ApJ, 426, 170
- Davidson, K., Kinman, T.D., 1985, ApJS, 58, 321
- deFreitasPacheco, J.A., Maciel, W.J., Costa, R.D.D., 1992, A&A, 261, 579
- Deharveng, L., Peña, M., Caplan, J., Costero, R., 2000, MNRAS, 311, 329
- Díaz, A.I., Pérez-Montero, E., 2000, MNRAS, 312, 130
- Dinerstein, H.L., 2001, ApJ, 550, L223
- Dinerstein, H.L., Geballe, T.R., 2001, ApJ, 562, 515
- Dopita, M. A., 1997, ApJ, 485, L41
- Dopita, M.A., Sutherland, R.S., 2000, ApJ, 539, 742
- Dopita,M.A., Vassiliadis,E., Wood,P.R., Meatheringham,S.J., Harrington,J.P., Bohlin,R.C., Ford,H.C., Stecher,T.P., Maran,S.P., 1997, ApJ, 474, 188
- Dreizler, S., Werner, K., 1993, A&A, 278, 199
- Dudziak, G., Péquignot, D., Zijlstra, A.A., Walsh, J.R., 2000, A&A, 363, 717
- Dwarkadas, V.V., Balick, B., 1998, ApJ, 497, 267
- Dwek, E., 1998, ApJ, 501, 643
- Elmegreen, B. G., 1998, in Abundance profiles: diagnostic tools for Galaxy History, Eds. D. Friedli et al., ASP Conference Series, Vol. 147, p. 279
- Escudero, A.V., Costa, R.D.D., 2001, A&A, 380, 300
- Esteban, C., 2002, in Ionized Gaseous Nebulae, Eds. W.J. Henney, J. Franco, M. Martos, & M. Peña (Conference Series of the Revista Mexicana de Astronomia y Astrofisica, vol. 12)
- Esteban, C., Peimbert, M, 1995, RMxAC, 3, 133
- Esteban, C., Peimbert, M., Torres-Peimbert, S., 1999, A&A, 342, L37
- Esteban, C., Peimbert, M., Torres-Peimbert, S., Escalante, V., 1998, MNRAS, 295, 401
- Esteban, C., Smith, L.J., Vílchez, J.M., Clegg, R.E.S., 1993, A&A, 272, 299
- Esteban, C., Vílchez, J.M., 1992, ApJ, 390, 536
- Esteban, C., Vílchez, J.M., Manchado, A., Edmunds, M.G, 1990, A&A, 227, 515
- Esteban, C., Vílchez, J.M., Manchado, A., Smith, L.J., 1991, A&A, 244, 205
- Esteban, C., Vílchez, J.M., Smith, L.J., Clegg, R.E.S., 1992, A&A, 259, 629
- Faundez-Abans, M., Maciel, W.J., 1986, A&A, 158, 228
- Faundez-Abans, M., Maciel, W.J., 1988, RMxAA, 16, 105
- Ferland, G.J., 2001, PASP, 113, 41
- Ferland, G.J. et al., 1996, in Analysis of Emission Lines, R. E. Williams & M. Livio (Cambridge: Cambridge Univ. Press), p. 83
- Ferland,G.J., Korista,K.T., Verner,D.A., Ferguson,J.W., Kingdon,J.B., Verner,E.M.,1998, PASP, 110, 761
- Ferland, G., Savin, D.W., 2001, Spectroscopic Challenges of Photoionized Plasmas, ASP Conference Series, vol. 247
- Fich, M., Silkey, M., 1991, ApJ, 366, 107
- Ford, H. C., 1983, in Planetary Nebulae, IAU Symposium no. 103, ed. D. R. Flower, p. 443
- Forestini, M., Charbonnel, C., 1997, A&AS, 123, 241
- Frank, A., Mellema, G., 1994a, A&A, 289, 937
- Frank, A., Mellema, G., 1994b, A&A, 430, 800
- Froese Fisher, C., Saha, H. P., 1985, Phys. Scri. 32, 181

- Galavís, M.E., Mendoza, C., Zeippen, C.J., 1997, A&AS, 123, 159
- Galli, D., Stanghellini, L., Tosi, M., Palla, F., 1997, ApJ, 477, 218
- García-Segura, G., Langer, N., MacLow, M.-M., 1996a, A&A, 316, 133
- García-Segura, G., MacLow, M.-M., Langer, N., 1996b, A&A, 305, 229
- García-Vargas, M.L., González-Delgado, R.M., Pérez, E., Alloin, D., Díaz, A., Terlevich, E., 1997, ApJ, 478, 112
- Garnett, D. R., 1992, AJ 103, 1330
- Garnett, D.R., Dinerstein, H.L., 2001, ApJ, 558, 145
- Gonçalves, D., Corradi, R. L. M., Mampaso, A., 2001, ApJ 547, 302
- GonzálezDelgado, R.M., Leitherer, C., Heckman, T.M., 1999, ApJS, 125, 489
- Górny, S. K. G., Stasińska 1995, A&A, 303, 893
- Górny, S. K. G., Tylenda, R., 2000, A&A, 362, 1008
- Greggio, L., Renzini, A., 1990, ApJ 364, 35
- Grevesse, N., Sauval, A.J., 1998, sce, conf, 161G Standard Solar Composition
- Gruenwald, R.B., Viegas, S.M., 1992, ApJS, 78, 153
- Gruenwald, R., Viegas, S.M., 1998, ApJ, 501, 221
- Gruenwald, R., Viegas, S.M., Broguière, D., 1997, ApJ, 480, 283
- Giveon, U., Sternberg, A., Lutz, D., Feuchtgruber, H., Pauldrach, A. W. A., 2002, ApJ, 566, 880
- Guerrero, M. A., Manchado, A., 1996, ApJ, 472, 711
- Guerrero, M. A., Manchado, A., Chu, Y.-H., 1997, ApJ, 487
- Gutierrez-Moreno, A., Moreno, H., 1988, PASP, 100.1497
- Harrington, J.P., 1968, ApJ, 152, 943
- Harrington, J.P., 1996, in Hydrogen-deficient Stars, Eds. C. S. Jeffery & U. Heber, ASP conf. ser. vol. 96, p. 193
- Harrington, J.P., Borkowski, K.J., Tsvetanov, Z.I., 1997, in Planetary Nebulae, IAU Symposium no. 180, eds. H. J. Habing and H. J. G. L. M. Lamers, p. 235
- Harrington, J.P., Feibelman, W.A., 1984, ApJ, 277, 716
- Harrington, J.P., Lutz, J.H., Seaton, M.J., Stickland, D.J., 1980, MNRAS, 191, 13
- Harrington, J.P., Marionni, P.A., 1981, in The Universe at Ultraviolet Wavelengths: The First Two Yrs. of Intern. Ultraviolet Explorer p. 623-631 (SEE N81-25893 16-90)
- Harrington, J.P., Seaton, M.J., Lutz, J.H., Adams, S., 1982, MNRAS 199, 517
- Henney, W.J., 1998, ApJ, 503, 760
- Henry, R.B.C., 1989, MNRAS, 241, 453
- Henry, R. B., C., 1993, MNRAS, 261, 306
- Henry, R.B.C., Kwitter, K.B., Bates, J.A., 2000, ApJ, 531, 928
- Herwig, F., 2000, A&A, 360, 952
- Herwig, F., 2001, in Post-AGB Objects as a Phase of Stellar Evolution, Eds. R. Szczerba & S. K. Górny, Kluwer, p. 249
- Hillier, D.J., Miller, D.L., 1998, ApJ, 496, 407
- Hoare, M.G., Roche, P.F., Glencross, William M., 1991 MNRAS. 251, 584
- Holweger,H., 2001, in Joint SOHO/ACE workshop "Solar and Galactic Composition". Ed. R. F. Wimmer-Schweingruber, American Institute of Physics Conference proceedings vol. 598, p.23
- Hou, J.L., Prantzos, N., Boissier, S., 2000, A&A, 362, 921
- Howard, J.W., Henry, R.B.C., McCartney, S., 1997, MNRAS, 284, 465
- Hubeny, I., Lanz, T., 1995, ApJ, 439, 875
- Hummer, D.G., Berrington, K.A., Eissner, W., Pradhan, A.K., Saraph, H.E., Tully, J.A., 1993,

A&A, 279, 298

- Hummer, D. G., Storey, P. J., 1992, MNRAS, 254, 277
- Hyung, S., Aller, L.H., Feibelman, W.A., 1994, PASP, 106, 745
- Hyung, S., Aller, L. H., Feibelman, W. A., Lee, W. B., de Koter, A., 2000, MNRAS, 318, 77
- Hyung,S., Mellema,G., Lee,S.-J., Kim,H., 2001, A&A, 378, 587
- Iben, I. Jr., Kaler, J.B., Truran, J.W., Renzini, A., 1983, ApJ, 264, 605
- Izotov, Y. I., & Thuan, T. X. 1998, ApJ, 497, 227
- Izotov, Y. I., Thuan T. X., & Lipovetsky, V. A. 1994, ApJ, 435, 647
- Jacoby, G.H., 1979, PASP, 91, 754
- Jacoby, G.H., Ciardullo, R., 1999, ApJ, 515, 169
- Jacoby, G.H., Ford, H.C., 1983, ApJ, 266, 298
- Jacoby, G.H., Morse, J.A., Fullton, L.K., Kwitter, K.B., Henry, R.B.C., 1997, AJ, 114, 2611
- Kaler, J.B., Iben, I.Jr., Becker, S.A., 1978, ApJ, 224L, 63
- Keyes, C.D., Aller, L.H., Feibelman, W.A., 1990, PASP, 102, 59
- Kingdon, J.B., Ferland, G.J., 1995, ApJ, 450, 691
- Kingdon, J.B., Ferland, G.J., 1996, ApJS, 106, 205
- Kingdon, J.B., Ferland, G.J., 1997, ApJ, 477, 732
- Kingdon, J., Ferland, G.J., Feibelman, W.A., 1995, ApJ, 439, 793
- Kingsburgh, R.L., Barlow, M.J., 1994, MNRAS, 271, 257
- Köppen, J., Acker, A., Stenholm, B., 1991, A&A, 248, 197
- Köppen, J., Cuisinier, F., 1997, A&A, 319, 98
- Koesterke, L., 2001, Ap&SS, 275, 41

Koesterke, L., Gräfener, G., Hamann, W.-R., 2000, in Thermal and Ionization Aspects of Flows from Hot Stars, ASP Conference Series, Vol. 204. Eds. H. Lamers & A. Sapar, p.239

- Krishnaswamy-Gilroy, K., Sneden, C., Pilachowski, C.A., Cowan, J.J., 1988, ApJ, 327, 298
- Kwitter, K.B., Henry, R.B.C., 1996, ApJ, 473, 304
- Kwitter, K.B., Henry, R.B.C., 1998, ApJ, 493, 247
- Lacy, J.H., Townes, C.H., Geballe, T.R., Hollenbach, D.J., 1980, ApJ, 241, 132
- Lamers, H. J.G.L.M., Nota, A., Panagia, N., Smith, L.J., Langer, N., 2001, ApJ, 551, 764
- Lattanzio, J., Forestini, M., 1999, in Asymptotic Giant Branch Stars, IAU Symposium no. 191, Eds. T. Le Bertre, A. Lèbre & C. Waelkens, p. 31
- Leisy, P., Dennefeld, M., 1996, A&AS, 116, 95
- Lennon, D.J., Burke, V.M., 1994, A&AS, 103, 273
- Lester, D.F., Dinerstein, H.L., Werner, M.W., Watson, D.M., Genzel, R., Storey, J.W.V., 1987, ApJ, 320, 573
- Leuenhagen, U., Hamann, W.-R., 1998, A&A, 330, 265
- Liu, X.-W., 1998, MNRAS, 295, 699
- Liu,X.-W., 2002, in Ionized Gaseous Nebulae, Eds. W.J. Henney, J. Franco, M. Martos, & M. Peña (Conference Series of the Revista Mexicana de Astronomia y Astrofísica, vol. 12)
- Liu,X.-W., Barlow,M.J., Cohen,M., Danziger,I.J., Luo,S.-G., Baluteau,J.P., Cox,P., Emery,R.J., Lim,T., Péquignot,D., 2001, MNRAS, 323, 343
- Liu, X.-W., Barlow, M.J., Danziger, I.J., Storey, P.J., 1995a, ApJ, 450, L59
- Liu, X.-W., Luo, S.-G., Barlow, M.J., Danziger, I.J., Storey, P.J., 2001, MNRAS, 327, 141
- Liu, X.-W., Storey, P.J., Barlow, M.J., Clegg, R.E.S., 1995b, MNRAS, 272, 369
- Liu,X.-W., Storey,P.J., Barlow,M.J., Danziger,I.J., Cohen,M., Bryce,M., 2000, MNRAS, 312, 585
- Luo, S.-G., Liu, X.-W., Barlow, M.J, 2001, MNRAS, 326, 1049

- G. Stasińska: Abundances in H II regions and planetary nebulae
- Luridiana, V., Cerviño, M., Binette, L., 2001, A&A, 379, 1017
- Luridiana, V., Peimbert, M, 2001, ApJ, 553, 633
- Luridiana, V., Peimbert, M., Leitherer, C., 1999, ApJ, 527, 110
- Lutz, D., Feuchtgruber, H., Genzel, R., Kunze, D., et al. 1996, A&A, 315, L269
- Maciejewski, W., Mathis, J.S., Edgar, R.J., 1996, ApJ, 462, 347
- Maciel, W.J., Köppen, J., 1994, A&A, 282, 436
- Maciel, W.J., Quireza, C., 1999, A&A, 345, 629
- Maeder, A., 1990, A&AS, 84, 139
- Manchado, A., Pottasch, S. R., Mampaso, A., 1988, A&A, 191, 128
- Marigo, P., 2001, A&A, 370, 194
- Marigo, P., Bressan, A., Chiosi, C., 1996, A&A, 313, 545
- Marston, A.P., 1997, ApJ, 475, 188

Marston, A.P., 1999, in Wolf-Rayet Phenomena in Massive Stars and Starburst Galaxies, IAU Symposium no. 193, Eds. K. A. van der Hucht, G. Koenigsberger & P. R. J. Eenens, p.306

- Marten, H., Szczerba, R., 1997, A&A, 325, 1132
- Martín-Hernández, N.L., Peeters, E., Morisset, C., Tielens, A.G.G.M., Cox, P., Roelfsema, P.R., Baluteau, J.-P., Schaerer, D., Mathis, J.S., Damour, F., Churchwell, E., Kessler, M.F., 2002, A&A, 381, 606
- Martins, L.P., Viegas, S.M., 2000, A&A, 361, 1121
- Mathis, J.S., 1983, ApJ, 267, 119
- Mathis, J.S., Liu, X.-W, 1999, ApJ, 521, 212
- Mathis, J.S., Rosa, M.R., 1991, A&A, 245, 625
- Mathis, J.S., Rumpl, W., Nordsieck, K.H., 1977, ApJ, 217, 425
- Mathis, J.S., Torres-Peimbert, S., Peimbert, M., 1998, ApJ, 495, 328
- McGaugh, S.S., 1991, ApJ, 380, 140
- McGaugh, S.S., 1994, ApJ, 426, 135
- Meatheringham, S.J., Dopita, M.A., 1991a, ApJS, 75, 407
- Meatheringham, S.J., Dopita, M.A., 1991b, ApJS, 76, 1085
- Medina, S., Peña, M., 2000, RMxAA, 36, 121
- Mellema, G., 1995, MNRAS, 277, 173
- Mellema, G., Frank, A., 1995, MNRAS, 273, 401
- Mendoza, C., 1983, in Planetary nebulae, IAU Symposium no. 103, Ed. D. R. Flower, Dordrecht, D. Reidel, p. 143
- Meyer, D.M., Cardelli, J.A., Sofia, U.J., 1997, ApJ, 490, L103
- Meyer, D.M., Jura, M., Cardelli, J.A., 1998, ApJ, 493, 222
- Middlemass, D., 1988, MNRAS, 231, 1025
- Middlemass, D., 1990, MNRAS, 244, 294
- Miller, Grant J., Chu, You-Hua, 1993, ApJS, 85, 137
- Monk, D.J., Barlow, M.J., Clegg, R.E.S., 1988, MNRAS, 234, 583
- Moore, B.D., Hester, J.J., Scowen, P.A., 2000, AJ, 119
- Morisset,C., Schaerer,D., Martín-Hernández,N.L., Peeters,E., Damour,F., Baluteau,J.-P., Cox,P., Roelfsema,P., 2002, A&A, 386, 558
- Nahar, S. N. , 2002, in Planetary nebulae and their Role in the Universe, IAU Symposium no. 209, in press
- Nahar, S.N., Pradhan, A.K., 1997, ApJS, 111, 339
- Nahar, S.N., Pradhan, A.K., Zhang, H. L., 2000, ApJS, 131, 375
- Najarro, F., Krabbe, A., Genzel, R., Lutz, D., Kudritzki, R.P., Hillier, D.J., 1997, A&A, 325, 700

- Napiwotzki, R., Heber, U., K"oppen, J., 1994, A&A, 292, 239
- Nota, A., Livio, M., Clampin, M., Schulte-Ladbeck, R., 1995, ApJ, 448, 788
- Nussbaumer, H., & Storey P., J., 1981, A&A, 99, 177
- Och,S.R., Lucy,L.B., Rosa,M.R., 1998, A&A, 336, 301
- O'Dell,C.R.,2001, PASP, 113, 29O
- O'Dell,C.R., Handron,K.D, 1996, AJ, 111, 1630
- O'Dell,C.R., Henney,W.J., Burkert,A, 2000, AJ, 119, 2910
- Oey,M.S., Kennicutt,R.C., Jr, 1993, ApJ, 411, 137
- Oey, M.S., Dopita, M.A., Shields, J.C., Smith, R.C., 2000, ApJS, 128, 511
- Oey,M.S., Shields,J.C.,2000, ApJ, 539, 687
- Oliva, E., Pasquali, A., Reconditi, M., 1996, A&A, 305, L21
- Olive, K.A., Skillman, E.D, 2001, New Astronomy, 6, 119
- Olive,K.A., Steigman,G., Skillman,E.D., 1997, ApJ, 483, 788
- Osterbrock, D. E., 1989, Astrophysics of Gaseous Nebulae and Active Galactic Nuclei (Mill Valley: University Science Books)
- Osterbrock, D., Flather, E., 1959, ApJ, 129, 26
- Osterbrock, D.E., Tran, H.D., Veilleux, S., 1992, ApJ, 389, 305
- Pagel, B.E.J., Edmunds, M.G., Blackwell, D.E., Chun, M.S., Smith, G., 1979, MNRAS, 189, 95
- Palla, F., Bachiller, R., Stanghellini, L., Tosi, M., Galli, D., 2000, A&A, 355, 69
- Patriarchi, P., Morbidelli, L., Perinotto, M., Barbaro, G. 2001, A&A, 372, 644
- Pasquali, A., Perinotto, M., 1993, A&A, 280, 581
- Pauldrach, A.W.A., Hoffmann, T.L., Lennon, M., 2001, A&A, 375, 161
- Peeters, E., Martín-Hernández, N.L., Damour, F., Cox, P., Roelfsema, P.R., Baluteau, J.-P., Tielens, A.G.G.M., Churchwell, E., Kessler, M.F., Mathis, J.S., Morisset, C., Schaerer, D., 2002, A&A, 381, 571
- Peimbert, M., 1967, ApJ, 150, 825
- Peimbert, M., 1978, in Planetary nebulae, IAU Symposium no. 76, Ed. Y. Terzian, Dordrecht, Reidel, p. 215
- Peimbert, M., 1990, Rep. Prog. Phys., 53, 1559
- Peimbert, M., 1996, in Analysis of Emission Lines, Eds. R. E. Williams & M. Livio (Cambridge: Cambridge Univ. Press), p. 165
- Peimbert, M., 2002, in Ionized Gaseous Nebulae, Eds. W.J. Henney, J. Franco, M. Martos, & M. Peña (Conference Series of the Revista Mexicana de Astronomia y Astrofisica, vol. 12)
- Peimbert, M., Carigi, L., Peimbert, A., 2001 Astrophys. Space Sci. Suppl., 277, 147-156
- Peimbert, A., Peimbert, M., Luridiana, V., 2002, ApJ (in press)
- Peimbert, M., Rayo, J.F., Torres-Peimbert, S., 1978, ApJ, 220, 516
- Peña,M., Stasińska,G., Esteban,C., Koesterke,L., Medina,S., Kingsburgh,R., 1998, A&A, 337, 866
- Peña, M., Stasińska, G., Medina, S., 2001, A&A, 367, 983
- Péquignot, D., 1986, in Model Nebulae (Publication de l'Observatoire de Paris)
- Péquignot, D., et al., 2002, in Ionized Gaseous Nebulae, Eds. W.J. Henney, J. Franco, M. Martos, & M. Peña (Conference Series of the Revista Mexicana de Astronomia y Astrofisica, in press)
- Péquignot, D., Baluteau, J.-P., 1994, A&A, 283, 593
- Péquignot, D., Petitjean, P., Boisson, C., 1991, A&A, 251, 680
- Péquignot, D., Stasińska, G., Aldrovandi, S.M.V., 1978, A&A, 63, 313
- Péquignot, D., Walsh, J.R., Zijlstra, A.A., Dudziak, G., 2000, A&A, 361, L1
- Pérez, E., 1997, MNRAS, 290, 465

- Perinotto, M., Bencini, C.G., Pasquali, A., Manchado, A., Rodriguez Espinosa, J.M., Stanga, R., 1999, A&A, 347, 967
- Perinotto, M., Kifonidis, K., Schoenberner, D., Marten, H, 1998, A&A, 332, 1044
- Perinotto, M., Panagia, N., Benvenuti, P., 1980, A&A, 85, 332
- Pilyugin, L.S., 2000, A&A, 362, 325
- Pilyugin,L.S., 2001, A&A, 369, 594
- Pottasch, S. R., 1984, Planetary Nebulae, Dordrecht, Reidel
- Ratag, M.A., Pottasch, S.R., Dennefeld, M., Menzies, J., 1997, A&AS, 126, 297
- Rauch,T., Deetjen,J.L., Dreizler,S., Werner,K., 2000, in Asymmetrical Planetary Nebulae II: From Origins to Microstructures, ASP Conference Series, Vol. 199. Eds. J. H. Kastner, N. Soker & S. Rappaport, p. 337
- Relaño, M., Peimbert, M., Beckman, J., 2002, ApJ, 564, 704
- Renzini, A., Voli, M., 1981, A&A, 94, 175
- Richer, M.G., 1993, ApJ, 415, 240
- Richer, M.G., McCall, M. L., 1995, ApJ, 445, 642
- Richer, M. G., McCall, M.L., Stasińska, G., 1998, A&A, 340, 67
- Richer, M.G., Stasińska, G., McCall, M.L., 1999, A&AS, 135, 203
- Rodríguez-Gaspar, J.A., Tenorio-Tagle, G., 1998, A&A, 331, 347
- Rubin, R. H., 1968, ApJ, 153, 761
- Rubin, R. H., 1989, ApJS, 69, 897
- Rubin, R.H., Dufour, R. J., Walter, D.K., 1993, ApJ, 413, 242
- Rubin, R.H., Simpson, J.P., Erickson, E.F., Haas, M.R, 1988, ApJ, 327, 377
- Rubin, R.H., Simpson, J.P., Haas, M.R., Erickson, E.F., 1991, ApJ, 374, 564
- Rubin,R.H., Simpson,J.P., Lord,S.D., Colgan,S.W.J., Erickson,E.F., Haas,M.R., 1994, ApJ, 420, 772
- Russell,S.C., Dopita,M.A., 1992, ApJ, 384, 508
- Samland, M., Köppen, J., Acker, A., Stenholm, B., 1992, A&A, 264, 184
- Sankrit, R., Hester, J.J., 2000, ApJ, 535, 847
- Sasselov, D., Goldwirth, D., 1995, ApJ, 444, L5
- Sauer, D., Jedamzik, K., 2002, A&A, 381, 361
- Savin, D.W., 1999, ApJ, 523, 855
- Schaerer, D., 2000, in Stars, Gas and Dust in Galaxies: Exploring the Links, ASP Conference Proceedings, Vol. 221. Eds. D. Alloin, K. Olsen, & G. Galaz, p.99
- Schaerer, D., deKoter, A., 1997, A&A, 322, 598
- Schmidt-Voigt, M., Köppen, J., 1987a, A&A, 174, 211
- Schmidt-Voigt, M., Köppen, J., 1987b, A&A, 174, 223
- Schöning, T., Butler, K., 1998, A&AS, 128, 581
- Searle, L., 1971, ApJ, 168, 327
- Seaton, M., 1987, J. Phys. B, 20, 6363
- Sembach, K.R., Savage, B.D., 1996, ApJ, 457, 211
- Shaver, P.A., McGee, R.X., Newton, L.M., Danks, A.C., Pottasch, S.R., 1983, MNRAS, 204, 53
- Shields, G.A., 1974, ApJ, 193, 335
- Shields, G.A., 1978a, ApJ, 219, 559
- Shields, G.A., 1978b, ApJ, 219, 565
- Shields,G.A., 1983, in Planetary nebulae, Proceedings of the IAU Symposium 103, Ed. D. R. Flower, Dordrecht, D. Reidel Publishing Co., p. 259
- Shields, J.C., Ferland, G.J., 1994, ApJ, 430, 236

- Shields, J.C., Kennicutt, R.C. Jr., 1995, ApJ, 454, 807
- Simpson, J.P., Colgan, S.W.J., Rubin, R.H., Erickson, E.F., Haas, M.R., 1995, ApJ, 444, 721
- Simpson, J.P., Rubin, R.H., 1990, ApJ, 354, 165
- Simpson, J.P., Witteborn, F.C., Price, S.D., Cohen, M., 1998, ApJ, 508, 268
- Skillman, E.D., 1989, ApJ, 347, 883
- Smith,L.J., 1996, in Wolf-Rayet stars in the framework of stellar evolution, Eds. J.M. Vreux, A. Detal, D. Fraipont-Caro, E. Gosset & G. Rauw, p.381
- Smits, D.P., 1996, MNRAS, 278, 683
- Sofia, U.J., Cardelli, J.A., Guerin, K.P., Meyer, D.M. 1997, ApJ, 482, L105
- Sofia,U.J., Meyer,D.M.,2001, ApJ, 554, L221, Sofia,U.J., Meyer,D.M. (erratum), 2001, ApJ, 558, 147
- Sembach, K.R., Savage, B.D., 1996, ApJ, 457, 211
- Spitzer, L., Jr., 1948, ApJ, 107, 6
- Spitzer, L. Jr., 1978, Physical Processes in the Interstellar Medium, John Wiley & Sons, New York
- Stasińska, G., 1980a, A&A, 85, 359
- Stasińska, G., 1980b, A&A, 84, 320
- Stasińska,G., 1998, in Abundance Profiles: Diagnostic Tools for Galaxy History, ASP Conf. Ser. Vol. 147, Eds. D. Friedli, M. Edmunds, C. Robert & L. Drissen, p. 142
- Stasińska, G., 2002, in Ionized Gaseous Nebulae, Eds. W.J. Henney, J. Franco, M. Martos, & M. Peña (Conference Series of the Revista Mexicana de Astronomia y Astrofisica, in press)
- Stasińska, G., Górny, S.K., Tylenda, R., 1997, A&A, 327, 736
- Stasińska, G., Izotov, Y., 2001, A&A, 378, 817
- Stasińska, G., Richer, M.G., McCall, M.L., 1998, A&A, 336, 667
- Stasińska, G., Schaerer, D., 1997, A&A, 322, 615
- Stasińska, G., Schaerer, D., 1999, A&A, 351, 72
- Stasińska, G., Schaerer, D., Leitherer, C., 2001, A&A, 370, 1
- Stasińska, G., Szczerba, R., 1999, A&A, 352, 297
- Stasińska, G., Szczerba, R., 2001, A&A, 379, 1024
- Stasińska, G., Tylenda, R., 1986, A&A, 155, 137
- Stasińska, G., Tylenda, R., Acker, A., Stenholm, B., 1992, A&A, 266, 486
- Stevenson, C.C., McCall, M.L., Welch, D.L., 1993, ApJ, 408, 460
- Storey, P.J., 1997, in Planetary Nebulae, IAU Symposium no. 180, eds. H. J. Habing and H. J. G. L. M. Lamers, p. 161
- Storey, P.J., Hummer, D.G., 1995, MNRAS, 272, 41
- Tamblyn, P., Rieke, G.H., Hanson, M. M., Close, L.M., McCarthy, D.W., Jr., Rieke, M.J., 1996, ApJ, 456, 206
- Torres-Peimbert, S., Peimbert, M., 1977, RMxAA, 2, 181
- Torres-Peimbert, S., Peimbert, M., Peña, M., 1990, A&A, 233, 540
- Tovmassian,G.H., Stasińska,G., Chavushyan,V.H., Zharikov,S.V., Gutierrez,C., Prada,F., 2001, A&A, 370, 456
- Tylenda, R., 1979, Acta Astronomica, 29, 355
- vandenHoek, L.B., Groenewegen, M.A.T., 1997, A&AS, 123, 305
- vanHoof,P.A.M., Beintema,D.A., Verner,D.A., Ferland,G.J.,2000, A&A, 354, L41
- Vassiliadis, E., Dopita, M.A., Bohlin, R.C., Harrington, J.P., Ford, H.C., Meatheringham, S.J., Wood, P.R., Stecher, T.P., Maran, S.P., 1996, ApJS, 105, 375
- Vassiliadis,E., Dopita,M.A., Bohlin,R.C., Harrington,J.P., Ford,H.C., Meatheringham,S.J., Wood,P.R., Stecher,T.P., Maran,S.P.,1998, ApJS, 114, 237

Vassiliadis, E., Dopita, M.A., Morgan, D.H., Bell, J.F., 1992, ApJS, 83, 87

Viegas, S.M., Clegg, R.E.S., 1994, MNRAS, 271, 993

Vílchez, J.M., Esteban, C., 1996, MNRAS, 280, 720

Volk,K., Dinerstein,H., Sneden,C., 1997, in Planetary Nebulae, IAU Symposium no. 180, Eds. H. J. Habing & H. J. G. L. M. Lamers, Dordrecht: Kluwer Academic Publishers, p. 284.

Walsh, J.R., Dudziak, G., Minniti, D., Zijlstra, A.A., 1997, ApJ, 487, 651

Walsh, J.R., Walton, N.A., Jacoby, G.H., Peletier, R.F., 1999, A&A, 346, 753

Webster, B.L., 1988, MNRAS, 230, 377

Weidemann, V., 1987, A&A, 188, 74

Weingartner, J. C., Draine, B. T., 2001, ApJ, 548, 296

Wen,Z., O'Dell,C.R., 1995, ApJ, 438, 784

Werner, K., 2001, Ap&SS, 275, 27

Zuckerman, B., 1973, ApJ, 183, 863